Journal of Scientific Research & Reports
4(4): 348-374, 2015; Article no.JSRR.2015.037
ISSN: 2320-0227

SCIENCEDOMAIN *international*
www.sciencedomain.org

The Magnetite-apatite Ore Deposit of Pınarbaşı (Bulam), Adıyaman Province, South-eastern Turkey

Hüseyin Çelebi[1*], Cahit Helvacı[2] and Ali Uçurum[3]

[1]Tatlısu Mahallesi, Akif İnan Sokağı 26, 34774 Istanbul, Turkey.
[2]Faculty of Engineering, Department of Geological Engineering, University of Dokuz Eylül, 35210 Alsancak, İzmir, Turkey.
[3]Faculty of Engineering, Department of Geological Engineering, Cumhuriyet University, 58140 Sivas, Turkey.

Authors' contributions

This work was carried out in collaboration between all authors. Author HÇ designed the study, wrote the protocol, and wrote the first draft of the manuscript, managed the literature searches, sampling and analyses of the study performed the spectroscopy analysis. Author CH conducted field work and text revision and author AU managed the geochemical analyses process. All authors read and approved the final manuscript.

Article Information

DOI: 10.9734/JSRR/2015/9793
Editor(s):
(1) Kal Renganathan Sharma, Energy and Manufacturing, Lone Star College, North Harris, USA and Department of Physics, College of Science and Technology,Texas Southern University Houston, TX 77004, USA.
(2) Masum A Patwary, Geography and Environmental Science, Begum Rokeya University Rangpur 5400, Bangladesh.
Reviewers:
(1) Kayode James Olatunji, Mineral Resources Engineering Department, Institute Of Technology, Kwara State Polytechnic, Ilorin, Nigeria.
(2) Anonymous, China university of geosciences(wuhan), China.
(3) Anonymous, University of Zanjan, Iran.
Complete Peer review History: http://www.sciencedomain.org/review-history.php?iid=743&id=22&aid=6605

Original Research Article

Received 28th February 2014
Accepted 16th September 2014
Published 23rd October 2014

ABSTRACT

The Precambrian (Pütürge Metamorphites), the Eocene (Maden Complex), the Permo-Carboniferous (Malatya Metamorphites), the tertiary conglomerates and the alluvial formation all crop out in the vicinity of the magnetite-apatite ore deposits of Pınarbaşı.
The Malatya Metamorphites, which are products of regional metamorphism in ore deposits, are in an area thrust over the Maden Complex. From bottom to top, the area includes chlorite schists, calc schists and recrystallized limestone. Abundant rock-forming minerals in the area include chlorite, mica, quartz and calcite. The existing mineral facies indicate that ore deposits in the area metamorphosed as at least one regional barrow type in the greenschist facies at 400°C

**Corresponding author: E-mail: ucurum@cu.edu.tr, huseyin.celebi@gmx.net, cahit.helvaci@deu.edu.tr;*

temperature and 0.4 MPa pressure, and they depend on contact and retrograde metamorphism. As a result of this process, the area's ore deposits are highly folded and faulted. The ores consist of magnetite, hematite (specularite) and goethite. The important gangue minerals are fluorapatite, quartz, chlorite and micas. Geologic and geochemistry data indicate that the original rocks of the recent chlorite schist were pelitic sediments.
Levels of the ^{18}O isotope showed that the formation temperature varied between 282-372°C. This temperature corresponds to the beginning of the greenschist facies temperature of the regional metamorphism. Hydrogen isotope analysis reflects the sedimentary rock's value and supports the geochemistry diagnosis. The radiometric age determination indicated two different age values, 66 and 48 Ma. The older age of 66 Ma explains the metamorphosis that evolved during the ophiolite development. The younger age of 48 Ma is interpreted as a second metamorphism, retrograde metamorphism or tectonic movement age.
The Pınarbaşı ore deposit is described as a metamorphosed metasedimentary magnetite-apatite ore deposit. Similar magnetite-apatite ore deposits is the Avnik deposits in Turkey. Determined proved and inferred reserves amount to 78 Mt with 35.07wt % Fe and 1.57wt % P_2O_5 content. The operation of the ore is currently planed for 2016.

Keywords: Pınarbaşı; magnetite-apatite; metamorphism; muscovite; quartz; geochemistry and geochronology.

1. INTRODUCTION

Magnetite-apatite ore deposits are one of the most important types of iron ores and encompass ore deposit types that are diverse both in derivation and in structure. This type of iron ore, which includes the Pınarbaşı magnetite-apatite ore deposit, is of great economic significance. The most important magnetite-apatite deposits in the world are the Kiruna/Sweden ore deposits [1], the Cerro de Mercado/Mexico [2,3,4] and Bafq/Iran [5,6]. In Turkey, this type of ore deposit is located in Bitlis Massif, Eastern Anatolia. These are the Avnik/Bingöl [7,8,9,10,11] and Ünaldı/Bitlis magnetite-apatite ore deposits [7,11].

The Pınarbaşı magnetite-apatite ore deposit is located approximately 6 km from Çelikhan in the Province of Adıyaman, Southeast Turkey. The study field, which is easily accessible, is reached via a 30 km asphalt road from Sürgü District on the Malatya-Gaziantep Highway (Fig. 1). The study area is about 10 km^2. Its altitude ranges between 1250 m (Zerban Spring) and 1670 m (Yayla). The field is characterized by profound, steep slopes which are barren of vegetation. The population density of the region is about 40 persons per km^2. In the vicinity of Pınarbaşı missing important industrial facilities. North of the Pınarbaşı, about 80 km, is the main Turkish Fe mining district Hasançelebi.

There have been numerous geologic studies of the study field and its vicinity [12,13,14,15,16]. In addition, the ore has been subjected to detailed geological investigation [17], analysis of its geochemical properties [18] and there have been combined studies of its geochemical, geochronological properties and economic investigation [19,20].

This study focused on analyzing which precious elements condense in the various ore, rock and mineral phases. It also examined the elements' economic potential and retrievability. In addition, the analyses of $^{18/16}O$ and ^{2}H isotopes were used to discover the atmosphere for ore formation, whereas the $^{40}Ar/^{39}Ar$ radioactive isotope analyses were used to determine the age of the deposits. Finally, the study examined the deposit's economic significance.

2. RESEARCH METHODS

2.1 Geology of the Study Area

The geological construction of Southeastern Anatolia is characterized by the Alpine orogenic segment in the north and the Arabian Platform in the south. These orogenic belt has been, from north to south, divided into three E-W tending structural zone [21]: 1. The napes zone, Late Cretaceous ophiolitic suite and metamorphic units of Paleozoic-Early Mesozoic age, 2. Imbricated zone of Late Cretaceous-Early Miocene age and 3. The sedimentary Arabian Platform, Early Cambrian-Middle Miocene [14] and [22].

2.1.1 Stratigraphic succession of the study area

In the near vicinity of the Pınarbaşı magnetite-apatite ore deposit occur rock units of various

ages and origin of above formations (Fig. 2). The lowermost unit of study area is the Pütürge Metamorphites Precambrian-Permian age [14,23] in eastern and are not to observe in deposit area. According to [24], [25,26] it is a part of Bitlis Massif and gained their present form in Eocene time. The lower contact of the unite is not observed, while upper contact is angularly unconformable with Eocene Maden Complex [27]. They display a prograde Berrovian-type regional metamorphism at amphibolite facies. They are well foliated and composed manly of gneiss, amphibolite schist, mica schist and recrystallized limestone.

The Permo-Carboniferous Malatya Metamorphites are the most common rocks of the deposit area and trust over the Maden Complex of Eocene age (Fig. 3). Their thickness reachs 1500 m. They comprise mainly metacarbonates and metapelites and turn slightly dark color (Fig. 4). The Malatya Metamorphites have a pronounced foliation and lineation (Fig. 5), tight folds and trust faults, [12,14] and divided it into Lower (chlorite schist, calc schist, quartzite and ore) and Upper Metamorphites (crystallized limestone). The calc schists of the chlorite schist formations are bituminous and dolomitic in places. The apatite-magnetite mineralizations of Pınarbaşı take place manly in this unit (Figs. 2 and 3).

The volcano-sedimentary Maden Complex of Eocene age is located with an angular discordance on the Pütürge Metamorphites [27]. In the upper contact the unit is thrusted by Malatya Metamorphites (Fig. 3). The Complex is best observed in the northeast area of the region and is composed of limestone of different colors, psammite of rough debris, pebble and clay stone intercalation of small debris, andesite, lithologies of diabase and splitic types [26]. The unit, which is as thick as 350 m, is slightly foliated under the effect of metamorphism. Its surface is composed of nummulite limestones [27].

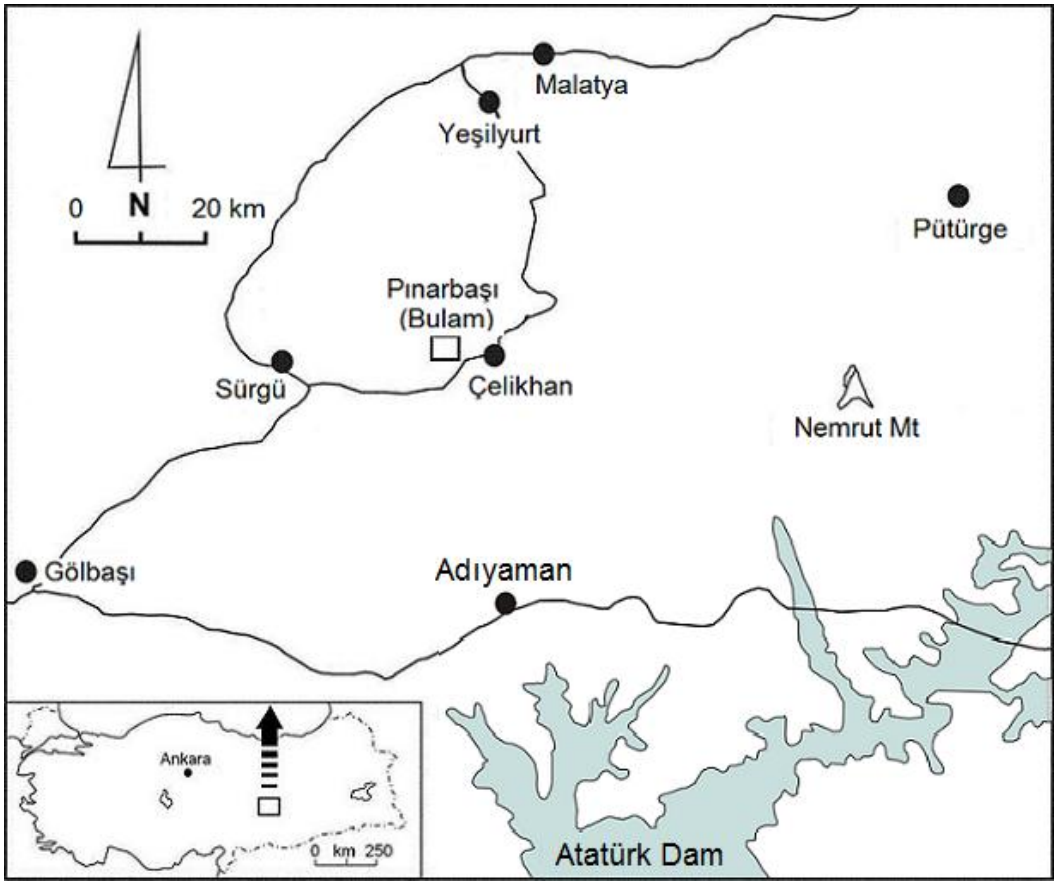

Fig. 1. Geographic location

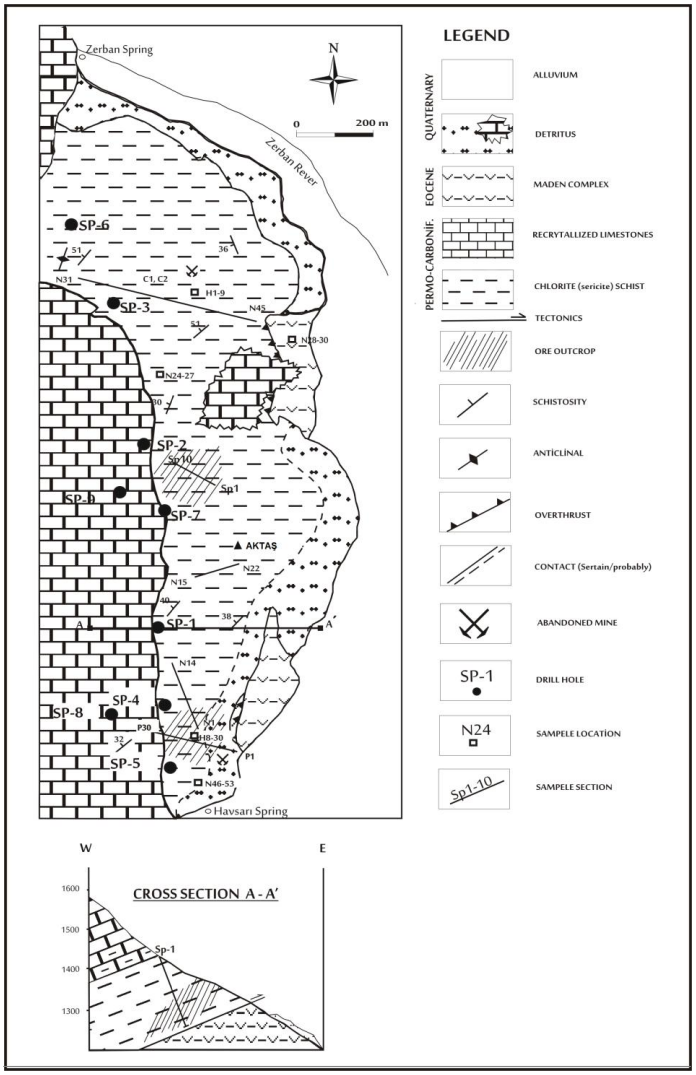

Fig. 2. Geological mape of the Pınarbaşı magnetite-apatite ore deposit (modified from Büyükkıdık and Aras, [17])

2.1.2 Tectonic setting

The most important structural elements of the study field are the overlaps and convolutions (Figs. 2 and 3). The field is greatly affected by tectonic movements because it is located on the collision belt of the Taurid Tectonic Belt with the Arabian Platform. The region was shaped by overlapping, normal and strike-slip faults while undergoing structural changes during various geological periods and evolution of the Southeastern Anatolia [28,29,14].

According to the field observations, the most important tectonic element of the ore deposit is the Şerefhan Overlapping Line, which passes south of the Pınarbaşı ore deposit (Fig. 3). The Malatya Metamorphites on the north, which are moving westward due to the collision of the Taurid Tectonic Belt with the Arabian Platform, have overlapped with the Maden Complex on the south. These events are due to north-south congestion resulting from the secondary pushes and slicing in the rock bodies. A secondary plane of schistosity due to the effect of deformation can be observed cutting across the main schistosity inside the rock. The ore has been substantially folded with the schists, which demonstrates that the ore formation is older than the deformation. The durable and solid ore lenses have reacted to deformation with fractures.

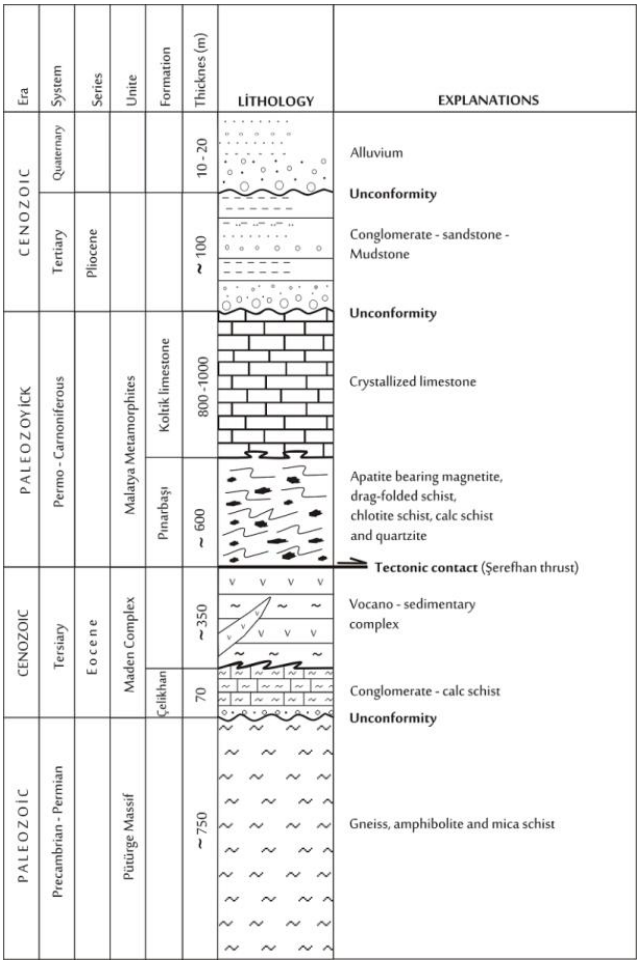

Fig. 3. Generalized stratigraphic columnar section of Çelikhan District (modified after Gözübol and Önal, [27] and Bozkaya et al. [14])

The ore area of the Pınarbaşı magnetite-apatite ore deposit, which is one of the most important of its kind in Turkey, covers an area approximately 300 m (east-west) wide and 2500 m (north-south) long. The Fe ore, consisting of magnetite and hematite, are bound to the chlorite schists of the Pınarbaşı Formation, which is located between the Maden Complex and recrystallized limestone (Fig. 2). Debris and alluviums occasionally cover ores on the surface.

2.1.3 Types and conditions of metamorphism

The rock bodies of the Pınarbaşı magnetite-apatite ore deposit and its vicinity have undergone at least one regional metamorphism with the greenschist facies. According to microscopic studies and mineral chemical analyses, the evident mineral paragenesis arising from the degree of metamorphism in Pınarbaşı are the chlorites (chloritoid), the micas (muscovite and biotite), the feldspar (albite, plagioclas), garnet (almandine) and the epidote (zoisite). The observed mineral assemblage pyrophyllite+chlorite+muscovite/chloritoid+biotite +garnet in the area provide the biotite zone (Çelebi et al., 2005a, see also Fig. 8) based on [30] of the greenschist facies of the regional metamorphism and it is characteristic for metapelites. The chemical analysis [19] show in ACF diagram [31] the quartz-albite-mucovite-chlorite sub-facies and Al-rich continental clay zone (see also Fig. 10a). The rarely biotite, epidote and garnet indicate that the metamorphism in Pınarbaşı reaches as far as the beginning of this sub-facies and that the regional metamorphism is of a barrowian type where the pressure is effectively rather weak. According to the mineral paragenesis and isotopic results (see 5.1 stable isotopes), the degree of

metamorphism corresponds approximately to 400°C and 0.4 GPa of pressure.

2.2 Mineralogical Background

2.2.1 Ore types and their properties

The ore, usually concentrating on the upper parts, is found as magnetite-apatite lenses or stratas (bands) at various levels [17,19]. Ore, developing vertically in the north-south overlapping direction, slides laterally and vertically with marble while it occurs with an angle of approximately 30° to the west (Fig. 2). The thickness of the ore lenses reach 15 m. They extend horizontally several 100 m. The ore stretches along with the wall rock to 200 m (Fig. 7). In massive, banded and disseminated forms, magnetite provides ore types of various structures and quality in terms of mineral concentrations. Only by the outside appearances and regardless of their genetic processes 3 ore types aredistinguished (for chemical composition see Table 1):

1. Massive ore is formed with a large amount of magnetite remaining from diminution of the wall rock (Figs. 5, 6 and 9). Here, the term “massive" includes the ores that have a Fe content of at least 60wt %. Massive ore, comprising approximately 10wt % of all ores, is common in the northern area of the ore deposit (Fig. 7). It is found more frequently on the upper levels. Therefore, Fe decreases with increasing depth. The massive ore, which indicates an obvious direction, is the type of ore with the highest concentration of P_2O_5 and is basically an indicator of a compatible slight correlation between apatite and magnetite (Fig. 13b).
2. Banded ore, which is better observed on the southern part of the deposit, varies in both depth and thickness. This ore, formed during metamorphism as well-oriented ore type, consists of alternating bands of magnetite, apatite and wall rock (Figs. 5 and 8). The thickness of the bands can reach 1 cm and varies according to the particle size of ore and gangue materials. Band formation develops in parallel to schistosity, and it shifts to disperse ores in the wall direction. The magnetite content of this type of ore is approximately 50wt %. In this ore, large and usually euhedral magnetite crystals prevail. Banded ore comprises about 40wt % of all ore.
3. Disseminated ore is the most common type of ore. It can be observed at various densities throughout the deposit, and it always accompanies banded and massive ores. However, the magnetite content of this ore does not exceed 30wt % and consists of irregular, thin, euhedral magnetite and apatite crystals that are rarely parallel to the direction of the schistosity. Therefore, only partial retrievability of this type of ore is possible.

Fig. 4. Malatya Matamorphites observed in the west of Pınarbaşı Village. Ore-bearing schists of Pınarbaşı Formation (middle, dark), Koltik Limestones (up, light; see also Fig. 3) and alluviums of Çelikhan Plain (front)

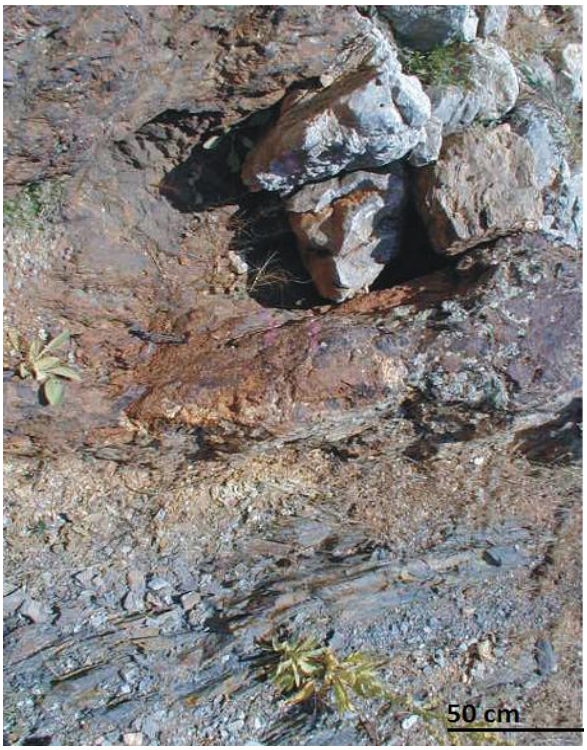

Fig. 5. Chlorite schist pronounced fibrous structure (below); limonitized, from banded to massive magenetite changing (middle, dark) (see also Fig. 6) and limestone blocks (above, light)

Fig. 6. Magnetite-apatite ore: Magnetite (dark) and apatit crystals (light) of different growth and directions with some chlorite on the bottom

The most common ore mineral of all this ore types is magnetite. This is followed by hematite and goethite. Among these, the specularite, which comprises as much as 30wt % of the rock, is the most common type of hematite. As accessory ore minerals occur ilmenite, rutile, siderite and psilomelane. The important gangue minerals are fluorapatite and quartz (Figs. 6 and 8). They are as aggregation or thin layer to find with magnetite. Apatite has a concentration varying generally between 3-5wt %. Its content reaches locally 60wt % on the northern part of the deposit (see also [17] and Fig. 7). Euhedral apatite crystals along the fractures and inclusions on the magnetite are occasionally observed [19] and [18]. Due its fine intergrowth (Ø<1 mm, Fig. 8) and its transparency, quartz is difficult to distinguish in the field. Rarely other phosphate minerals also occur,for example xenotime and monazite.

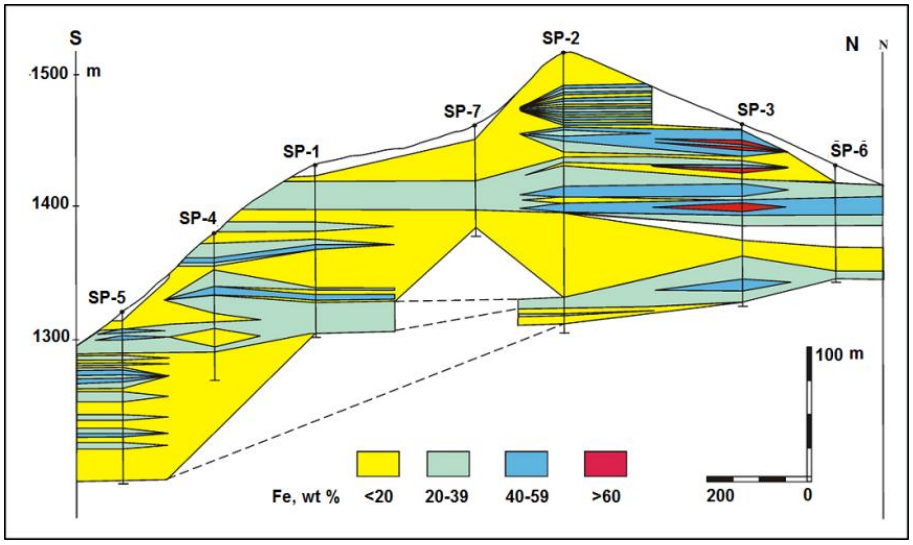

Fig. 7. N-S cross section thrugh the ore body shows the horizontal seting, however the ore is situated deeper in the south part of the deposit (see also corresponding holes in Fig. 2). The massive ore is concentrated in upper and northern areas of the deposit

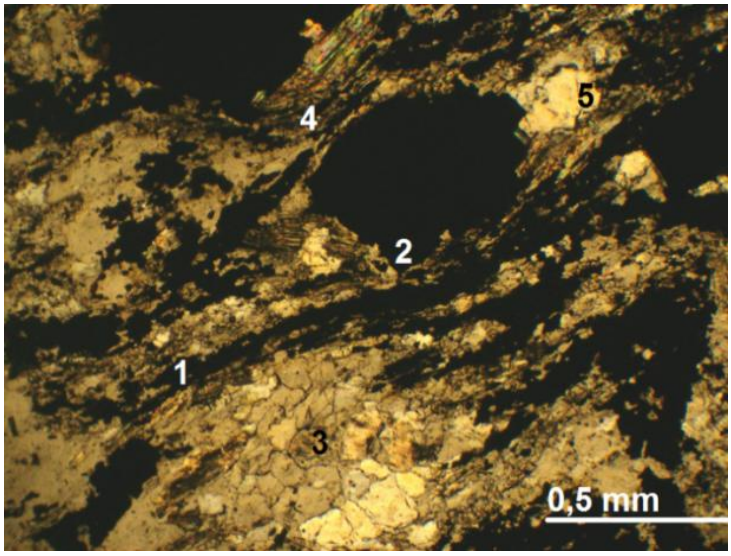

Fig. 8. Ore-wall rock relation: Parallel to schistosity well ordered and fine grained ore (hematite/specularite) 1, idiomorphic premetamorphism magnetite 2, fine grain apatite 3, chlorite fibres 4 and quartz 5, crossed nicols. The ore minerals are bound to chlorite schists

2.2.2 Microscopic investigations

Mineralogical studies have show that the wall-rock mineral composition of the Pınarbaşı magnetite-apatite ore deposit is not complex. The wall rock minerals are generally well oriented or cut as a result of the directed forces (i.e., stress) of the metamorphism. These characteristics reveal that the main rocks of the deposit did not differ greatly during metamorphism.

The most common minerals of the wall rock are green-grey chlorite and light-brown mica (Figs. 5 and 8). The majority of variously sized particles consist of chlorites (easily distinguished by their fibrous structure) and mica minerals (having a lamina shape), followed by quartz (Fig. 8). Magnetite and apatite, which are the precious

minerals of the deposit, are bound to chlorite and mica (Figs. 5 and 8). Semi-euhedral chlorites demonstrate a cleavage in a single direction. They are easily distinguished by their faded greenish color, low optical unevenness and blue-grey weaving. The mica with cleavage in a single direction (muscovite and biotite) is traced as euhedral minerals parallel to the schistosity, and they demonstrate strong pleochroism. Rare hornblendes are occasionally well developed [19]. Quartz usually has a wavy deflation and is non-euhedral. The ore developing along the schistosity plane (specularite) can be traced in large poicoblasts along the cracks that formed along the schistosity planes. In addition, small amounts of plagioclase, epidote/allanite, zircon, tourmaline, calcite, dolomite and opaque minerals can be traced.

The magnetite particles of Pınarbaşı, which may be as small as 0.5 mm in the rich or massive ore zones, can reach several millimeters in diameter in the dispersed ores (Figs. 8 and 9). Magnetite is usually non-euhedral. Euhedral magnetite crystals can be found in the non-directed, dispersed ores that have been slightly affected by the tectonism. Hematite, which surrounds the gangue minerals as a specularite in the hematite samples, can be found as a matrix in samples where it is present with magnetite (Fig. 9). Here, the intensive martitization of magnetite along the cracks can be observed as xenoblast, indicating that the magnetite was present in the rock prior to metamorphism and indicating that hematite established the cement of the rock. It has a pure composition and their V concentration is clearly less than 0,5 wt % and those of Ti, Mn and Co is lower still [19]. Resistant magnetites that were formed prior to metamorphism do not conform to the direction imposed by metamorphism.

There is no authentic hematite ore formation in Pınarbaşı. The hematite on the surface has partially transformed into goethite. Usually found as martite that is the product of magnetite oxidation. Martite formation has developed in two directions along the magnetite octaeder walls. On the surface, martite formation is enhanced on the cracks and breaches, and specularite was formed as lamellite, which is the second representative of hematite [19,17].

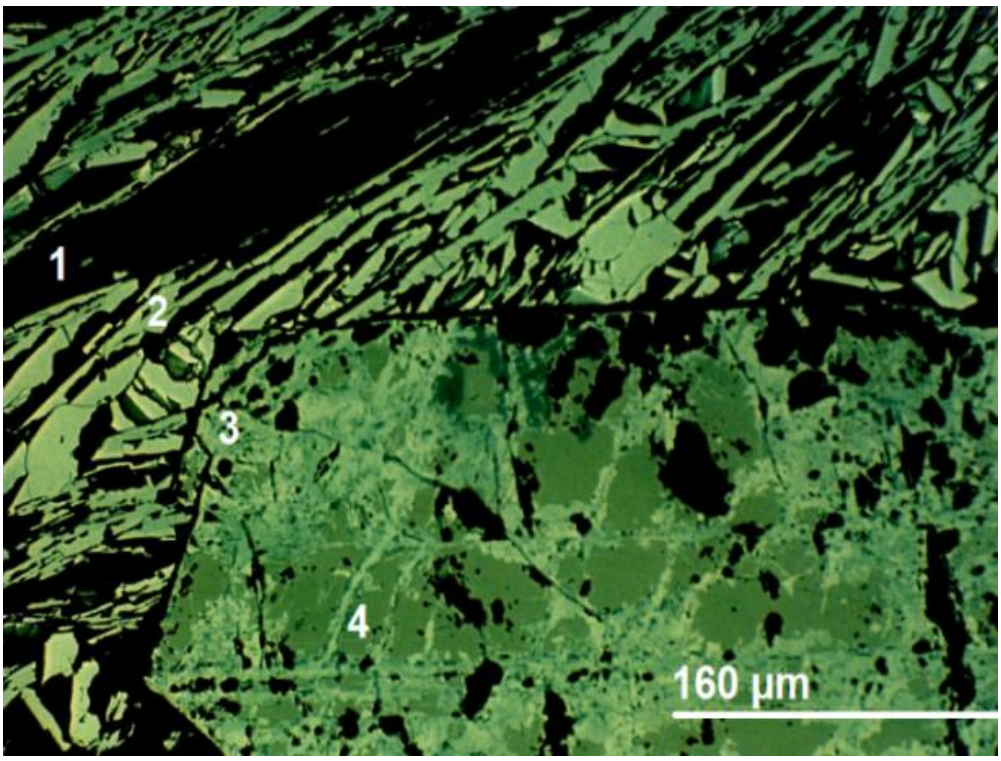

Fig. 9. Pure magnetite and hematite intergrowth. Chlotrite matrix 1, well ordered hematites (specularite) acrossed by idiomorphic magnetite crystal 2, idiomorphic magnetite crystal 3 and intensive martitisation along the fractures 4, parallel nicols

3. INTERPRETATION OF THE RESULTS

3.1 Sampling and Analytical Methods

Geochemical search studies on the Pınarbaşı magnetite-apatite ore deposit were based on the samples taken from sections indicated in (Fig. 2) and on the values determined from nine drilling analyses. The calculations demonstrated that about 80 samples were enough to provide 95wt % reliability (meaningfulness) for the analytical results. 154 rock and ore samples, each weighting about 2 kg, were taken randomly from various rock/ore bodies in the study area. Of those, 107 samples were composed of ore (this means: FeO content>20wt %), and 47 samples of whole rock, were largely taken from fresh ore and wall rock. After halving the samples were first ground to a 200 µm particle size for the classification process. The material was determined by the separation of mono-mineral samples ground less than <100 µm.

To purify it from closures and mixtures, pure mineral samples were separated into mineral parts using a mineral reagent following wet sieving and drying. After foreign matter was sorted using binoculars, the mono mineral samples were ground to <100 µm particle size for analysis. Analyses of all rock elements were conducted at the Technical University of Berlin (TUB) in the geochemical laboratories of Institute für Lagerstaettenforschung. The X-RAY method (the Philips brand, powder-1 program) was used and utilized 5 g powder tablets in a vacuum. Here, 40 main and trace elements in 75 samples were analyzed. The distribution of the samples that were analyzed was summarized according to the type of rock and mineral (see also [19]):

Type of samples	Number of samples	Mineral	Number
Rock		Magnetite	5
Whole rock	16	Apatite	6
Quartz schist	2	Allanite	1
Calc schist (dolomite)	3	Xenotime	3
Ore		Monazite	2
Magnetite-apatite	51	Chlorite	1
Hematite-apatite	1	Quartz	3
Goethite	2	Muscovite	2
Total	**75**		**23**

Analytical values of the representative basis for the elements detected on these samples are provided in (Table 1). Among the trace elements that were analyzed, the concentration of Ag, As, Bi, Br, Cl, Cs, Hg, Mo, Sb, Se, Sn, Tl and W was below the detection limit (<10 ppm). The elements Cd, Cr, Ga, Sn and U were not detected at reliable concentrations. The platinum group elements (PGE) were not found in these samples. However, the Au concentration reached 1 ppm.

Analyses of magnetite and all rock REEs, as well as rare elements such as Sc, Hf, Nb and Ta, were conducted via inductively coupled plasma examination (using an ICP-ES9 at the ACME Analytical Laboratories Ltd./Canada and using a REE microprobe at the Bundesanstalt für Geowissenschaften und Rohstoffe, BGR, Federal Republic of Germany).

Radiogenic isotope analyses (i.e., $^{40}Ar/^{39}Ar$, in muscovite) were conducted at the laboratories of the University of Michigan (USA), according to [32]. Stable isotope analyses (i.e., $^{18}O/^{16}O$, ^{2}H, muscovite, magnetite and quartz) were conducted at the Institute of Geological and Nuclear Sciences Ltd./New Zealand (according to [33,34,35]).

3.2 Wall Rock Geochemistry

The most obvious feature of the wall-rock analysis of Pınarbaşı ore deposit is the high concentrations of total Fe (averaging 14.22wt %) and P_2O_5 (0.32wt %). In addition, the concentration of many trace elements such as Ba, Sr, Zn and Zr is high, whereas that of elements such as Na, K, Rb and Cu is low. These rocks, which have an average SiO_2 content of 52.15wt %, have an Al_2O_3 concentration of 17.31wt %. According to the standard deviation value for these components, the samples exhibit a homogenous distribution. However, the distribution of MgO and K_2O is rather variable. Analysis values of certain samples representing these rocks are provided in (Table 1). These data indicate that the common quartz schists and dolomitic limestones are rather pure.

Table 1. Chemical analyses of selected whole rocks and ore samples (X-ray analyzes)

	Whole rocks					Ore				
	Chlorite schist			Quartz sch. dolomite		Magnetite-apatite			Specularite goethite	
	Ch-6	N-7	P-17	N-18	N-11	N-8	P-23	Sp-5	N-44	G-1
Oxides [wt %]										
SiO_2	44.77	52.37	56.82	85.26	2.50	17.08	29.91	35.90	8.04	19.27
TiO_2	0.97	1.10	1.16	0.35	nd[1]	0.32	0.34	0.53	0.27	0.39
Al_2O_3	15.52	24.95	23.29	3.07	2.41	9.73	9.34	7.68	7.49	10.81
Fe_2O_3*	16.38	11.24	8.61	5.73	2.23	61.37	39.66	40.62	68.40	62.12
MgO	9.94	1.79	0.67	nd	13.71	<0.30	0.40	0.78	<0.30	0.53
CaO	4.59	0.93	1.55	0.29	34.28	4.00	10.24	4.46	7.08	1.55
Na_2O	4.05	1.20	0.46	nd	0.85	0.27	0.22	0.47	0.45	nd
K_2O	0.47	3.02	2.67	nd	1.15	1.53	1.41	0.17	1.48	1.60
P_2O_5	0.15	0.10	0.27	0.24	0.09	2.87	6.62	4.32	5.97	1.25
MnO	0.13	0.05	0.06	0.02	0.11	0.18	0.08	0.18	<0.02	0.52
SO_3	0.03	0.02	0.02	0.01	nd	0.07	0.03	0.03	0.15	0.05
V_2O_3	<0.05	<0.05	<0.05	<0.05	<0.05	0.12	0.30	<0.05	0.27	0.14
F	<0.08	<0.08	<0.08	<0.08	<0.08	<0.08	0.08	0.34	0.64	0.17
H_2O	0.65	0.05	0.60	0.12	0.16	0.03	0.07	0.13	0.04	[2]na
CO_2	2.16	4.24	1.83	0.95	41.93	1.20	0.55	2.99	0.36	na
Sum	**98.81**	**101.06**	**98.09**	**96.04**	**99.42**	**98.77**	**99.14**	**98.60**	**100.64**	**98.40**
Trace elements [ppm]										
Ba	119	355	325	62	<30	352	285	21	227	346
Co	16	<10	35	67	nd	17	13	125	<10	43
Cr	<30	521	253	<30	nd	116	156	40	98	<30
Cu	16	10	27	<10	nd	<10	<10	<10	<10	<10
Ni	<12	110	20	<12	nd	90	49	94	37	32
Pb	<15	92	22	<15	<15	27	<15	76	<15	<15
Rb	<10	108	91	nd	nd	67	42	62	78	nd
Sr	225	271	76	nd	89	469	237	241	361	90
Th	<10	14	<10	nd	nd	18	<10	<10	<10	<10
Zn	53	116	156	nd	nd	110	40	178	<40	229
Zr	81	226	264	310	nd	232	121	299	197	156
Elemet ratios										
Ba/Rb	3.3	3.6								
Ca/Sr	145	120	429							
Ni/Co			0.6			5.3	3.8	0.6		0.7
Ti/V	32	55	58	35		4.6	11.3	18	1.8	7

**Total iron oxide;1nd: Not dedected;2na: Not analyzed*

The rocks of basic character were most likely derived from sedimentary rocks. This view is supported by quartzites and schales occur from the field [19]. Such a well defined direction of magmatic rocks can only be explained by a high degree of metamorphism. However, Pınarbaşı demonstrates only a low- or medium-degree of metamorphism conditions. Moreover, the works of other researchers [14] and [26] and geochemical data present the clues about the sedimentary rocks, i.e. metapelites, including the following:

- The position of the analysis values on the alk-al-c/fm diagram (Fig. 10a) and the variation of the Niggli-mg and Niggli-c in diagram of [36] correspond to pelitic sediments (Fig.10b).
- The significant negative correlation of incompatible elements (MgO, Cr, Ni, and Co) with SiO_2 and the elements' poor positive correlation between each other [19]. This character indicates a sedimentary differentiation,
- The high content of Al, Ba and Rb and the presence of a higher ratio of K to Na (K/Na= 2.52, [19], compare also Table 1),
- The positive correlation of K_2O-Ba (Fig. 11a, r^2= 0,86), Al_2O_3-Ba (Fig. 11b, r^2=0,50) and K_2O-Al_2O_3 (Çelebi et al., 2005a,

r^2=0,26). This correlation results from the binding of the above mentioned elements to the clay minerals,

- The low content of Cr, Ni, Ti and V (Table 1) compared to that of basic rocks and
- Alkaline rocks have a Sr/Ba ratio >1(basalts:1,8) [37]. Pınarbaşı other hand, has a Sr/Ba ratio of 0,60 [19]. This supports the sedimentary origin.

The correlation analysis confirms the results of the alk-al-c/fm, Niggli-c-Niggli-mg values and their sedimentary origin in (Fig. 10a and b). The element correlations of the sample material examined here from the wall rock indicate that there is a significant correlation between many pairs of elements, that the chlorite schists are saturated with these elements and that their origins were sedimentary rocks. This is exemplified by the significant positive correlation between K_2O and Al_2O_3, K_2O-Ba and Al_2O_3-Ba. In parallel to these main components, there are similar correlations between trace elements, such as the significant K_2O-Rb correlation (r^2=0,94) that results from the replacement of rubidium in K minerals [19].

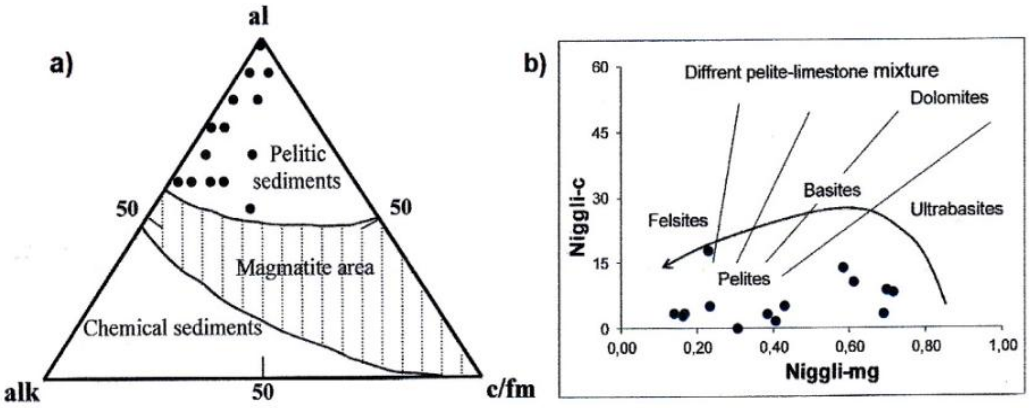

Fig. 10. Distribution of alk-al-c/fm values of whole rock in alk-al-c/fm triangle a), and variation of Niggli-mg and Niggli-c values in comparison of different rocks b), [36] (see text)

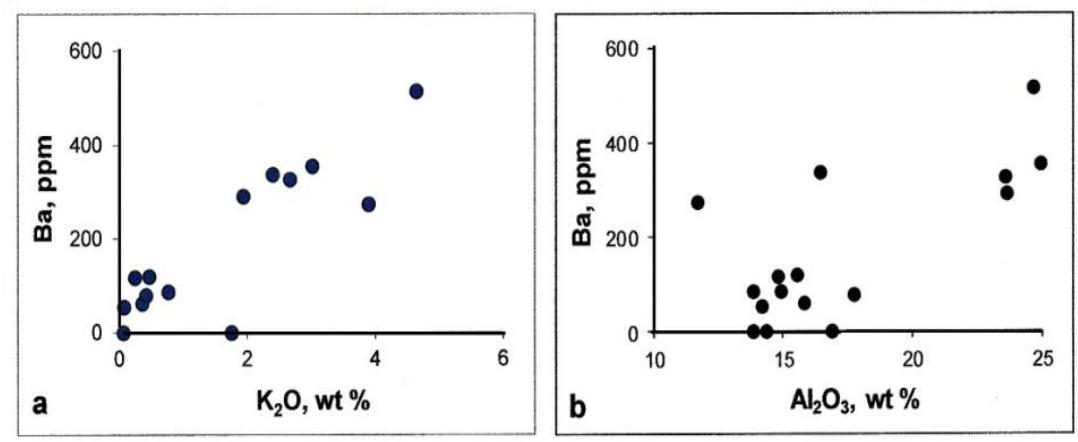

Fig. 11. Correlation between K_2O-Ba and Al_2O_3-Ba of whole rock (n=16). Scattering based on distribution of elements in different minerals such as chlorides, micas and magnetite. Significant correlation coefficient |r|>0,62 for P=.99 statistical confidence

3.3 Ore Geochemistry

The magnetite-apatite ore samples of the Pınarbaşı ore deposit are poor in terms of side and trace elements. Analysis values of some representative ore samples (FeO>20wt %) are provided in (Table 1). The most important feature of the samples is their richness in terms of iron (Fe) and phosphorus (P) and their poverty in terms of alkali elements (Na and K), earth alkali elements (Mg and Ca) and trace elements (Co and Ni).

The main component of the ore samples that were analyzed is the Fe (average 51.61wt % FeO= 37.16wt % Fe) that results from magnetite and the Si (24.65wt % SiO_2) that results from silicates (chlorite and mica). The average value of P_2O_5 as a precious raw material is 3.02wt % (approximately 1.29wt % P) [19]. This value is high enough to negatively affect the processing of iron because concentrations of P < 0.05wt % are required for the production of steel. However, P can be separated [38,39,40].

The FeO and Al_2O_3 values demonstrate the most stable distribution, whereas all other components are variable. These features indicate that the deposit has an almost homogenous ore formation. This is also reflected in the Al_2O_3-TiO_2 distribution in (Fig. 12) for expression that point to sedimentary rocks [41]. This means a low Ti content and suggests a sedimentary origin. A precise average management tenor can be attained during any possible management.

The siderophile elements, with regard to the Clarke value [37,42], are enriched in the deposit, whereas the alkali elements Na and K and earth alkali elements Mg, Ba and Sr become impoverished (Table 1) [19]. Phosphorus is the most concentrated element (by approximately 17-fold), followed by Fe (10-fold), F (8-fold) and V (5-fold). Hematite (specularite) is very poor in terms of trace elements. However, the chemical composition of goethite samples is parallel to the composition of ore. All elements, except for Fe and Zn, have become substantially less frequent with regard to basalts. The low H_2O content can be attributed to dehydration during the prograde metamorphism (see also [18]).

There are significant correlations between concentrations of element pairs of the samples analyzed. The most obvious negative correlation is observed between SiO_2, FeO and P_2O_5, which establish the magnetite and apatite precious raw materials. These properties indicate that the silicates, alkali and other main elements were thinned with the concentration of FeO and P_2O_5. For example, although FeO and SiO_2 concentrations (r^2=0.76) demonstrate a significant negative correlation (Fig. 13a). On the other hand the correlations between SiO_2 and TiO_2, Al_2O_3, MgO and F are positive because of their silicate phase [19]. There is no significant correlation (r^2=0.01) between FeO and P_2O_5(Fig. 13b). In fact, the high phosphorus concentration causes the low concentration of iron and dispersion of the high P_2O_5 concentrations. This context is in the holes with r^2=0.25 significantly positive [19]. FeO and P_2O_5 are negatively correlated with depth. (Fig. 7) also confirms this correlation.

The positive correlation between FeO and V_2O_3 (r^2=0.25) (Fig. 13c) shows that the V in magnetite first replaced Fe^{2+} (0.072 nm) as V^{3+} (0.074 nm) and not reached its saturation point in the media. According to [19] there is no link between P_2O_5 and F. That is, that F was bound to mica, in addition to apatite, for example, to muscovite and biotite as well, and the O^{2-}, Cl^-, OH^- and CO_3^{2-} ions partially replaced F, too. Finally the correlation between P_2O_5 and V_2O_3 (r^2=0.19) is better than that of P_2O_5 and F (r^2=0.01), see also [19]. This means that even in the apatite V is enriched. The highly meaningful and concordant CaO-P_2O_5correlation in (Fig. 13d) (r^2=0.83) indicates that the media is saturated in Ca and that it was completely gathered in apatite.

The total concentration of rare earth elements (REEs) in the Pınarbaşı magnetite-apatite ore deposit is 530 ppm (Table 2). The highest concentration is observed in Ce. Normalized REE distribution, according to chondrites, is presented in (Fig. 14a). All samples exhibit a similar REE distribution, an obvious separation and a slight negative Eu anomaly. Similar REE distributions indicate that ore formation in the deposit is the product of a single function. The negative Eu anomaly is attributed to high O_2 fugacity [43,44]. Extensive separation results from the more enrichment of heavy REEs relative to light REEs. For example, a ratio of La/Yb=3.6 indicates that there is poor separation of heavy REEs—this ratio is 28 in Kiruna [1]. In extensive separation, the La/Yb ratio can exceed 100.

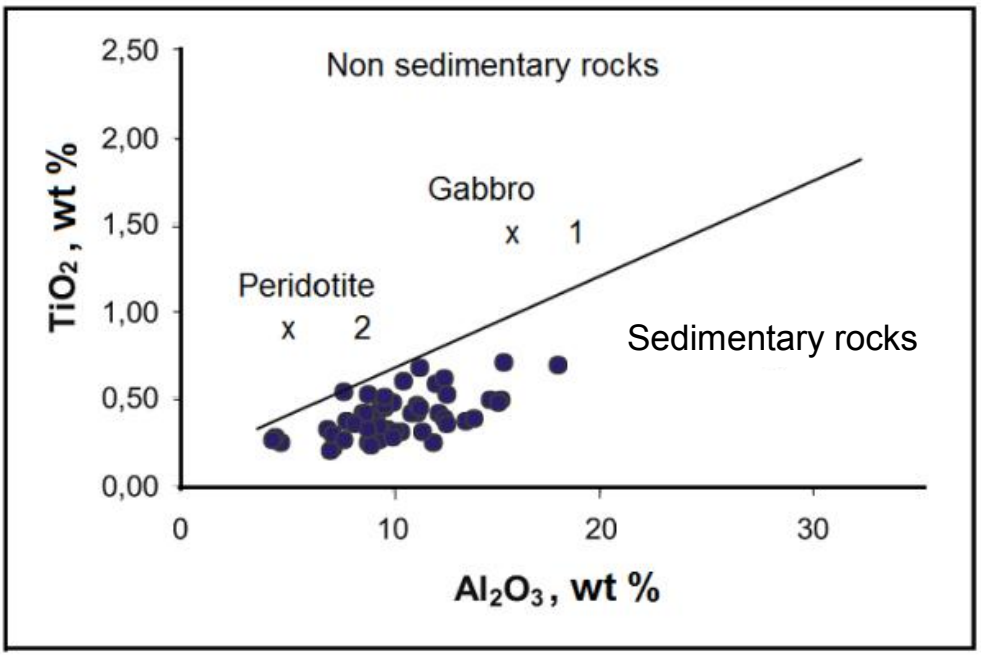

Fig. 12. Variation of Al_2O_3-TiO_2 values in comparison of sedimentary and nonsedmentary rocks (see text). 1 Paleozoic and Mesozoic oolitic iron rocks and 2 current iron-rich oolits of Lake Chad [41]

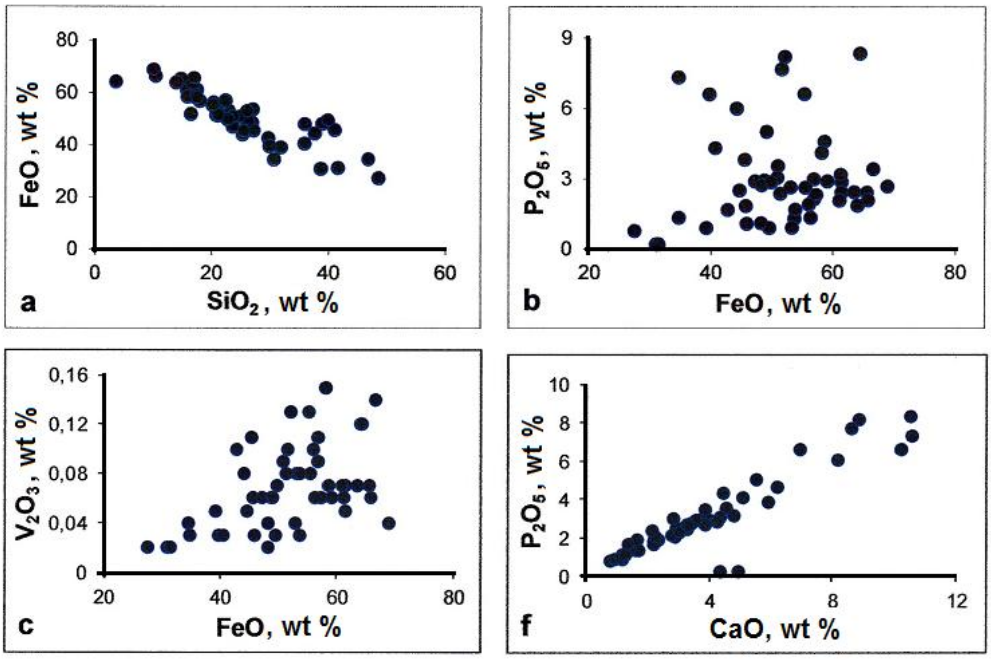

Fig. 13. Correlation between important element pairs in magnetite-apatite ore (n=51). Scattering based on distribution of different elements such as chlorides, micas and magnetite. The higher values of P_2O_5 an V_2O_3 are more dispersed. Significant correlation coefficient |r| > 0,27 for P=.99 statistical confidence (see text)

Table 2. Concentration of REEs in selected magnetite-apatite ore samples and averages of chondrites [42] (see also Fig. 14a, b)

REEs [ppm]	N-8	N-39	N-47	P-23	Mean	Chondrites
La	62.1	140.2	51.4	64.0	78.5	0.245
Ce	82.4	325.7	113.2	211.0	204.5	0.638
Pr	21.3	38.5	13.2	20.7	23.0	0.096
Nd	88.9	150.9	47.6	68.3	93.3	0.474
Sm	25.9	38.3	10.5	24.9	24.3	0.154
Eu	5.9	9.0	1.7	6.3	5.8	0.058
Gd	27.6	39.7	8.8	29.5	26.0	0.204
Tb	5.7	7.1	1.6	5.5	5.0	0.037
Dy	32.5	38.1	8.8	29.9	26.8	0.254
Ho	6.6	8.2	1.8	6.2	5.8	0.057
Er	18.7	23.0	5.3	16.7	15.8	0.166
Tm	3.0	3.4	0.8	2.3	2.3	0.026
Yb	19.8	21.3	5.4	13.6	14.8	0.165
Lu	2.9	3.2	0.8	1.9	2.3	0.025

The distributions of REEs in ore, magnetite and apatite are compared in (Fig. 14b). The ore and apatite distribution are similar to each other because of the poor Ce anomaly and the slight REE enrichment. The magnetite has a low content of REEs. The apatites, in which heavy REEs are more concentrated than the light ones, are distinguished from these. More enrichment of the heavy REEs in apatite probably comes from the crystal size of apatite. The REEs are more advantageous in terms of energy than Ca^{2+} (0.108 nm), so light REEs with large radii (e.g., Ce^{3+}, 0.109 nm) were replaced by heavy REEs with small radii (e.g., Yb^{2+}, 0.95 nm), see also [42].

3.3.1 Magnetite geochemistry

The analysis values and significant statistical criteria for the with a magnetic separator purified and ICP-ES analyzed five representative magnetite samples are provided in (Table 3). The samples have a relatively high TiO_2 and V_2O_3 content, and their concentration of MnO and trace elements is low and stable. These characteristics confirm the view that the magnetite is pure, and they demonstrate that the ore types have significant common features. Their $FeO+MnO+TiO_2+V_2O_3$ content averaged 95.86wt % (69.37wt % Fe+Mn+Ti+V). For comparison the theoretical highest Fe content of magnetite is 72.4wt % [45]. Accordingly, the Fe content of Pınarbaşı magnetite is high. This is due to the fact that magnetite is not saturated with trace elements, for example, because of low grade metamorphism [30,37].

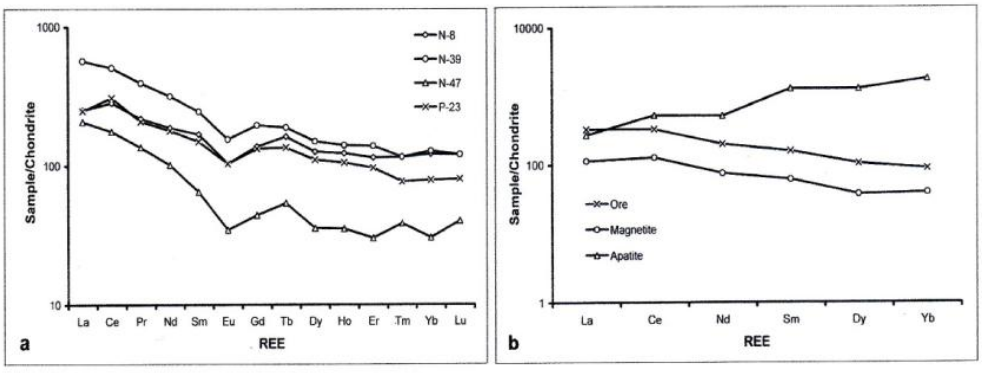

Fig. 14. Distribution of chondrite normalized REEs concentraions in representative magnetite-apatite ore samples a, and in different phases of ore b. Average ore samples (n=4), magnetite (n=5) and apatite (n=4) (see also Tables 2, 4, 5 and Fig. 15 and 16)

Low Th and U concentrations indicate that these elements prefer the apatite phase. The levels of trace elements such as Co, Cr and Ni (which are beneficial for steel production) or harmful elements such as As and S were not considered to be significant. However, the high concentration of 0,47 P_2O_5 (0.21wt % P) (Table 3) indicates that apatite has micro-particles (<100 μm) as inclusion in magnetite, as well as microscopic findings confirm [19,18]. This character complicates magnetite processing in advanced phases. For example, it increases the concentrate cost, which includes reducing P levels to less than 0.05wt %, as required by blast furnace applications.

The crystal cell dimension of Pınarbaşı magnetite has been measured as follows:

a_0=0.8387 nm (P-1) and
a_0=0.8394 nm (P-23).

The value of these dimensions in the literature is a_0=0.8396 nm [46]. Based on the average values provided in (Table 3), the general formula of Pınarbaşı magnetites is approximately equal to the following:

$$Fe^{2+}_{0.997}(Mg, Mn, Ni, Zn\ etc.)_{0.003}O^{2-}.\ Fe^{3+}_{1.971}(Al, Cr, Mn, Ti, V, etc.)_{0.029}O^{2-}_{3}$$

This result proves that the magnetite is quite pure. The largest mixture is established by SiO_2 (1.25wt %), which can hardly intrude the crystal structure of magnetite. Therefore, this content largely stems from contamination. The average V concentration of 800 ppm is rather low for magnetite. The V concentrations are higher in magnetites from similar deposits, such as metamorphic Avnik (Turkey, 900 ppm) [10] (Sweden, 1200 ppm) and magmatic El Laco (Chile, 1360 ppm) [47]. The magnetites of Pınarbaşı are poorer in terms of trace elements than the magnetite-apatite ores with magmatic origins. The same characteristics are exhibited by the element ratio. For example, the Ti/V ratio (0.95) is lower than ores with magmatic origins such as Avnik (1.70), Mishdovan (2.05) and Cerro de Mercado (3.20). However, the Cr/Ni ratio is as high as 1.60 (respectively, 0.10; <1.00, [48]; 0.26; [49,5].

Table 3. Chemical composition and trace elements concentration of selected magnetite samples

Oxides [wt %]	N-24	P-1	P-16	P-18a	P-23	Av.±stand. dev.
SiO_2	2.55	3.55	0.91	1.39	2.84	2.25±1.08
TiO_2	0.12	0.22	0.08	0.15	0.07	0.13±0.06
Al_2O_3	0.95	1.84	0.59	0.98	0.56	0.98±0.52
FeO*	95.90	89.82	98.36	97.00	96.79	95.57±3.33
MnO	0.07	0.05	0.03	0.02	0.02	0.04±0.02
V_2O_3	0.11	0.17	0.12	0.11	0.10	0.12±0.03
MgO	0.09	0.05	0.02	0.04	0.02	0.04±0.03
CaO	0.36	1.36	0.19	0.12	0.37	0.48±0.50
Na_2O	0.01	0.01	0.05	0.01	0.02	0.02±0.02
K_2O	0.08	0.02	0.04	0.08	0.08	0.06±0.03
P_2O_5	0.38	1.18	0.23	0.18	0.37	0.47±0.41
H_2O	-1.20	-1.50	-1.40	-0.70	-1.50	-0.66±1.25
Sum	**99.42**	**99.77**	**99.22**	**99.38**	**99.74**	**99.50**
Trace elements [ppm]						
Ba	33	6	13	27	15	15±9
Co	36	6	22	25	38	23±13
Cr	41	82	48	54	75	65±16
Cu	1	24	1	1	1	6±9
Ni	44	22	32	50	56	40±16
Sr	37	44	24	11	19	25±14
Th	17	15	13	12	5	12±5
U	1	3	1	2	2	2±1
Y	51	102	55	30	36	56±33
Zn	64	30	26	38	16	28±9
Zr	141	107	159	93	79	110±35
Element ratios						
Ti/V	1.41	1.20	0.96	0.59	0.62	0.95
Cr/Ni	0.93	3.73	1.50	1.08	1.34	1.70

*Total iron oxide

Magnetites are regarded as poor in terms of REEs that are normalized according to chondrites. The total REE concentration in Pınarbaşı magnetites is less than 200 ppm (Table 4). Magnetites of similar ores, such as Kiruna 2000 ppm [1] and Avnik have REE concentrations greater than 500 ppm [8], respectively. These low concentrations indicate that REEs in the Pınarbaşı magnetites have not reached saturation. This is in line with the low concentration of trace elements listed above. In addition, the REEs' preference for the apatite phase should also be considered. The REE distribution in the selected samples is stable, which supports the claim of homogenous magnetite composition.

In the Pınarbaşı magnetites, the light REEs are more concentrated than the heavy REEs. The first four light REEs (i.e., La, Ce, Pr and Nd) comprise 75wt % of the total REE concentration. However, the average ratio of La/Yb (3.89) is low, which indicates that the elements did not decompose well (Fig. 15a). This ratio is 1.48 in chondrites and is approximately 30 in Avnik. A significant positive La-Ce correlation also suggests a significant positive ΣNTE-(Th+U) correlation [19]. These data suggest that for REE and U to move in Pınarbaşı, the complex compositions of CO_3^{2-} and F^- were significant [44].

In the REE distribution of Pınarbaşı magnetites that were normalized according to chondrites, a small Eu negative anomaly can be observed (Fig. 14a and 15a). This weak anomaly indicates a high O_2 mobility. High O_2 mobility causes the oxidation of Eu^{2+} (0.121 nm) to Eu^{3+} (0.109 nm; [50]), thus causing a shift to early phases. Therefore, the Eu content thins in the last phases of crystallization and cannot enrich. Because apatite is present as an early phase, the negative Eu anomaly is more obvious than the negative Eu anomaly in the magnetite. In the distribution, a slightly positive Ce anomaly is observed, which indicates that Ce is found in the media with 4+ valences. The Ce anomaly also indicates that seawater is not effective because it leads to a negative Ce anomaly [1].

When the REE distribution in Pınarbaşı is compared to magnetites of similar deposits in Turkey, Avnik (Bingöl Province) and Ünaldı (Bitlis Province), one can observe that the differentiation in Pınarbaşı is slight, that the negative Eu anomaly is small and that heavy REEs are better concentrated (Fig. 15b). These observations demonstrate that the magnetite-apatite ore formation in Pınarbaşı is different from those of deposits of Bitlis Massif. This finding is supported by the new results described here.

Table 4. Concentration of REEs in selected magnetite samples, compared with those of the magnetite-apatite ore deposits of Turkey, Avnik and Ünaldı, (see also Fig. 15a, b)

REEs Pınarbaşı Avnik Ünaldı Chondr [ppm]									
Chondrites samples	**N-24**	**P-1**	**P-16**	**P-18a**	**P- 23**	**Mean**	**(n=3)**	**(n=3)**	**[42]**
La	23	58	21	22	11	26.92	55.33	126.50	0.245
Ce	70	149	58	69	49	78.68	88.00	217.00	0.638
Pr	7	17	7	7	4	8.41	6.67	19.00	0.096
Nd	30	71	30	27	17	34.80	17.00	53.50	0.474
Sm	9	19	8	7	4	9.46	2.00	7.00	0.154
Eu	2	4	2	1	1	2.07	0.15	0.40	0.058
Gd	9	19	8	6	5	9.43	1.44	5.59	0.204
Tb	2	3	2	1	1	1.75	0.24	0.84	0.037
Dy	10	18	10	5	6	9.70	1.22	4.38	0.254
Ho	2	4	2	1	1	2.08	0.25	0.87	0.057
Er	6	10	7	3	4	5.90	0.64	2.33	0.166
Tm	1	1	1	1	1	0.98	0.11	0.35	0.026
Yb	7	11	8	4	4	6.76	0.81	2.31	0.165
Lu	1	2	1	1	1	1.10	0.14	1.73	0.025
La/Ce	0.33	0.39	0.36	0.32	0.22	0.34	0.63	0.58	0.38
La/Yb	3.29	5.27	2.63	5.50	2.75	3.89	68.30	54.54	1.48

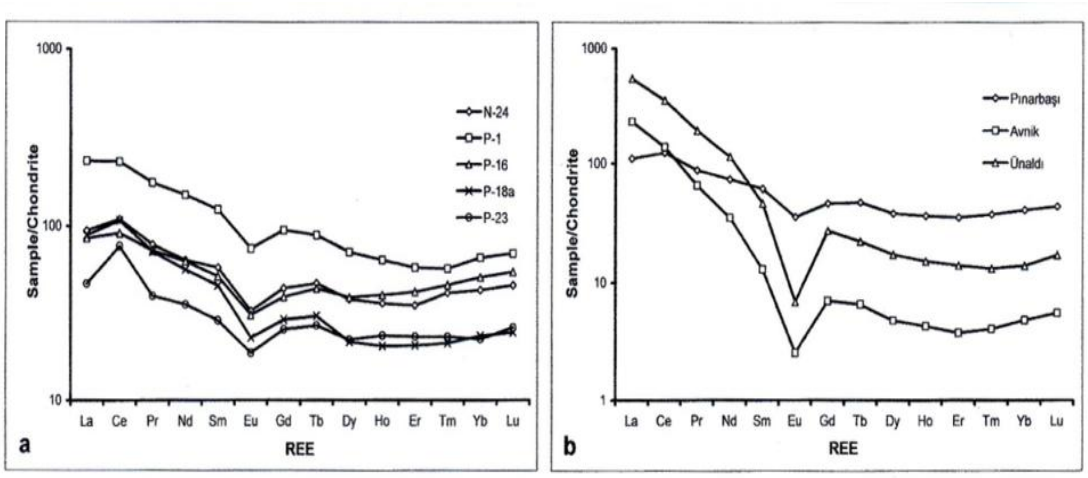

Fig. 15. Distribution of chondrite normalized REE concentrations in magnetites: Pınarbaşı magnetites a, and magnetites of similar magnetite-apatite ore deposits of Turkey b, (see also Table 4)

3.3.2 Apatite geochemistry

The apatite in the Pınarbaşı magnetite-apatite ore deposit is fluor apatite. The apatite content only rises rarely above 30wt %, and it is found in cm size (Fig. 6) to micro-particles smaller than 100 µm (Fig. 8), along with magnetite ore. The off-white apatite does not demonstrate any radioactivity and does not exhibit obvious luminescence. These features indicate a low content of trace elements (i.e., U, Th and REEs).

Fluor concentrations in Pınarbaşı apatite vary between 2.0-4.3wt %. Fluor apatite, $Ca5[F/(PO_4)_3]$, theoretically contains 55.60wt % CaO (39,74 Ca), 42.22wt % P_2O_5 (18.43wt % P) and 3.77wt % F [46]. Pınarbaşı apatites contain approximately 54.85wt % CaO, 42.21wt % P_2O_5 and 3.65wt % F (Table 5). The difference from the theoretical value comes from the displacement of elements. The analyzed samples exhibited a homogenous composition, and significant differences were only observed in the F, Fe and Y concentrations. Significant trace elements include SrO, FeO and Y_2O_3.

Apatite is an important component of magmatic and metamorphic rocks. An important part of the Ca ions in its structure are coordinated by oxygen in a coordination of six, and another part of those ions are coordinated in a coordination of seven by fluor, chlorine and hydroxyl ions through oxygen [43]. Therefore, in the crystal cell, the elements Ca, P and F can be replaced by many trace elements. Primarily, Mg, Mn, Ti and rare earth elements replace Ca. Phosphorus is replaced by Si, S, V, As and CO_3. Fluorine is replaced by O, Cl, and OH ions (-O≡0.42 F).

The approximate formula of the apatites was calculated on the basis of the obtained element concentrations. [51] uses the items 10A, 6Z and 26X in the calculation of the apatite formula. In this study, these items are represented as follows:

A=Ca, Ce, Mg etc.,
Z=P, S, As etc. and
X=O, F, Cl etc.

Based on the analysis values provided in (Table 5), the aforementioned items can be approximately calculated as follows:

10A ≈ 9.786 Ca; 0.076 Fe; 0.047 Sr; 0.075 Y; 0.016 Ce,
6Z ≈ 5.882 P; 0.002 Al; 0.003 S; 0.009 Si and
26X ≈ 22.05 O; 3.88 F; 0.07 Cl.

Then, the approximate chemical formula of the Pınarbaşı apatites is as follows:

$$Ca^{2+}_{4.89}(Fe, Y, Sr, Ce\ v.\ s.)_{0.11}[F^{1-}_{1.94}\ (Cl, OH)_{0.03}/P^{5+}_{2.94}(Al, S, Si\ v.\ s.)_{0.06}]\ O^{2-}_{11.03}$$

Table 5. Composition and REEs concentrations of selected apatite samples compared with those of the Avnik [8], Durango [50] and Nile-Phosphorites [52] (see also Fig. 16)

	Oxides Pınarbaşı							
Samples	**N-5**	**N-44**	**P-22b**	**P-23**	**Av.±stand. dev.**	**Avnik**	**Durango**	**Nile-[wt %] phosph**
CaO	56.20	55.72	56.47	55.87	56.07±0.34	55.94	54.02	38.61
P_2O_5	42.25	41.77	41.41	41.76	41.80±0.34	41.71	40.78	24.89
F	3.14	3.65	3.57	3.47	3.46±0.22	3.63	3.53	2.34
Cl	0.03	0.02	0.01	0.01	0.02±0.01	0.10	0.41	nd[1]
SiO_2	0.04	0.10	0.02	0.03	0.05±0.04	0.23	0.34	0.08
Al_2O_3	0.01	0.01	0.01	0.01	0.01±0.00	nd	0.07	0.42
FeO*	0.45	0.44	0.64	0.20	0.43±0.18	0.13	0.06	1.91
SO_3	0.01	0.05	0.01	0.01	0.02±0.02	0.16	0.37	2.21
SrO	0.20	0.24	0.24	0.24	0.23±0.02	0.12	0.07	0.15
ThO_2	0.01	0.02	0.01	0.02	0.02±0.01	nd	0.02	nd
Y_2O_3	0.01	0.21	0.15	1.18	0.39±0.53	0.12	0.10	0.01
O≡F,Cl	-1.33	-1.54	-1.50	-1.46	-1.46±0.09			
Sum	**101.01**	**100.67**	**101.03**	**101.32**	**101.01**	**100.80**	**99.77**	**70.62**
REEs [ppm]								
La	43	128	43	43	64±43	371	2900	77
Ce	85	299	85	85	139±107	824	4519	124
Nd	43	214	86	86	107±74	568	1190	65
Sm	87	87	87	87	87±00	197	132.5	15
Dy	131	174	131	131	142±22	196	69.2	15
Yb	132	132	86	132	121±22	93	31.3	9
Element ratios								
La/Ce	0.51	0.43	0.51	0.51	0.49	0.13	0.64	0.62
Ce/Yb	0.64	2.27	0.99	0.64	1.14	8.87	144.38	13.78

**Total FeO; [1]not dedected*

This apatite formula shows that the apatites analyzed here have a quite pure mineralogical composition. The Y, Sr and REE concentrations replacing Ca are not high. However, the concentrations of Cl and OH replacing fluor are very low. Additionally, the concentrations of Al, As, S, Si and V replacing P are very low. Therefore, it is not be meaningful to focus on the heavy metal trace elements because of their low concentration and the number of samples. For Pınarbaşı apatites, only Ba (approximately 500 ppm), Cr (300 ppm) and Zr (175 ppm) are interesting because of their high concentration in certain samples. Again, the low concentration of trace elements can be associated with a poor degree of metamorphism and with the low concentration of these elements in the main rock (i.e., the sedimentary rocks).

The fluor content and the crystal cell constants show that the Pınarbaşı apatite, with the chemical formula provided above, is fluor apatite. These constants (expressed in nm) and their ratios are calculated as follows:

P-23 sample	**N-21 sample**
a_0=0.9407	a_0=0.9485
c_0=0.6886	c_0=0.6781
c_0/a_0=0.732	c_0/a_0=0.732

Here the c_0 values are low, whereas the a_0 values are high. High c_0 (c_0>0.689 nm) and low ao values for sedimentary apatites, and low c_0 but high a_0 (a_0<0.940 nm) values are determinant [53]. In the Pınarbaşı apatites, the c_0/a_0 ratio is as low as 0.732, which supports the sedimentary hypothesis.

For the comparison of composition of the Pınarbaşı apatites with that of the apatites from other magnetite-apatite deposits –Avnik [8] and Durango [50] - and the composition of the Nile-Phosphorites [52] is provided in (Table 5). The Pınarbaşı apatites are similar to magmatic apatites of Avnik and Durango with regard to the main components (i.e., Ca, P and F). However, significant differences are observed with regard to the low concentrations of Cl and SO_3 and with regard to the high SrO concentration. The Pınarbaşı apatites are quite poor in trace elements and REEs when compared to the other deposits. In Nile-Phosphorites,

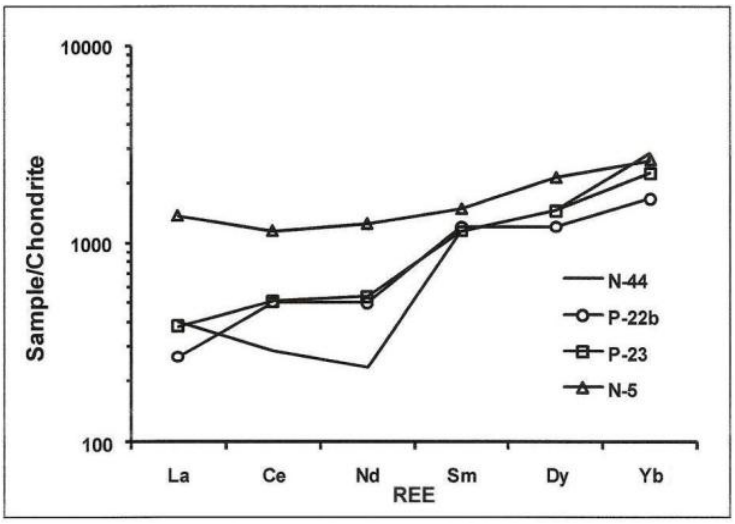

Fig. 16. Distribution of chondrite normalized REE concentrations in apatite samples (see Table 5)

however, the concentrations of FeO and SO_3 are quite high, which distinguishes them from all of the provided types of apatite. The Nile-Phosphorites with a low F content have the same SrO and REE concentrations as the Pınarbaşı apatites. Their element ratios are also the same. The analyzed apatites appear similar to the sedimentary Nile-Phosphorites.

When normalized according to chondrites, the distribution of detected REEs in apatites demonstrates an increase from light to heavy (i.e.,La-Lu, Fig. 16). This result reveals that heavy REEs preferably concentrate in apatite. Most likely, it is easier for REEs with small ion radii to intrude the crystal structure of apatite. The same situation is also observed in xenotime. This mineral, which contains 5wt % Dy_2O_3 and 4.2wt % Yb_2O_3, has La, Ce and ThO_2 concentrations below 0.10wt %. For the geochemical properties of apatite similar minerals, such as monazite (i.e., La-Ce-Th[PO_4]), xenotime (i.e., Y[PO_4]) and allanite (i.e., orthite=Ce-epidote), is here to [54] referenced.

4. ISOTOPES GEOCHEMİSTRY

4.1 Stable Isotopes Geochemistry: $^{18}O/^{16}O$, ^{2}H

Mineral association in the Pınarbaşı magnetite-apatite ore deposit showed that the best method for temperature detection is by examination of the oxygen isotopes. For example, the ^{18}O isotope is at its highest concentration in the oxygen compounds of Si-O-Si. In contrast, magnetite contains the least ^{18}O isotope [37,55]. Because the high difference in isotopes will yield good results, a selection of methods was used with consideration of these oxides' distribution in the field along with the speed, precision and cost-effectiveness of the analysis method. In addition, easy separation of these phases makes it easy to obtain the required sample material with necessary features and in necessary amounts.

In the chlorite-quartz-magnetite-apatite compound that was randomly collected on the field for isotope analyses, samples of rock/ore weighing approximately 1 kg were ground to a particle size of 250 µm in a chrome carbide grinder. Following wet sieving in 250-100 µm sieves, the sample material was washed with pure water and was first sorted with a handheld magnetic separator to remove magnetite and mafic minerals. The material was then sorted under a microscope for particles of magnetite and quartz of 20 g each. This sorting was also used to separate muscovite lamellites for analysis. Magnetite and quartz oxygen isotopes were used for the analysis of formation temperature, and muscovite was used for radiometric age detection and H isotope analyses [19].

Oxygen isotope analyses were conducted with a Micromass IsoPrime mass spectrometer with a Eurovector 3000 analyzer at the University of Nevada-Reno, Department of Geological

Sciences, Laboratory of Stable Isotope Geochemistry. The relative error rate for the method is ±0.15‰. The δ values were calculated according to the equality of quartz-magnetite phases:

$$1000 \ln \alpha = D\frac{10^6}{T^2} + E\frac{10^3}{T} + F \quad (1)$$

Here D=1.220, E=8.220 and F=-4.35 [56,57].

The temperatures obtained varied between 372.8-282.4ºC. These are the temperatures that were at minimum reached during the metamorphism when the muscovite was formed. In the deposit, the formation of biotite, magnetite and garnet indicate that a higher temperature was attained due to pressure. This issue shall be a subject of future studies.

The results obtained here confirm the temperature-pressure conditions detected via mineral paragenesis [31,30]. It is concordant with mineral associations that were optically detected, to the metamorphic conditions and to the rocks that are related products. It is not meaningfully different from 415°C, which represents the greenschist facies of 370°C metamorphism (a difference of 12wt %). The same values correspond to sedimentary rock isotope values detected for quartz and magnetite in certain resources. For example, the $\delta^{18}O$ values of magmatic quartz vary between 8.9–10.3 wt %, whereas those of magnetite vary between 1.0-3.0 wt %. In Pınarbaşı, these values are above 17 wt % and 2.6 wt %, respectively, and they are similar to the values of sedimentary rocks. The $\delta^{18}O$ values of quartz conflict with those of pelitic schists (12-18 wt %; [58]). The isotopes were probably re-balanced as a result of recrystallization that developed through metamorphism.

The δD values of the analyzed P-09 sample (-53 wt % VSMOW) also indicates rocks with sedimentary origins. However, while the Pınarbaşı values provided in both figures are far from seawater values, δD values reflect an atmospheric water contamination in the region. Studies on fluid inclusions may develop an approach to the issue.

4.2 Radiogenic Isotopes Geochemistry: $^{40}Ar/^{39}Ar$ Dating

The Ar-Ar age-detection method is a modified version of K-Ar age detection method. The method is based on the principle of transforming ^{40}K through neutron bombardment into ^{39}Ar. The reaction is as follows:

$$^{39}_{19}K + n \rightarrow ^{39}_{18}Ar + p \quad (2)$$

Thus, the n amount of main isotope is indirectly detected through ^{39}Ar, instead of via direct detection through ^{40}K. Therefore the main and daughter isotopes need not be detected through distinct methods, as in the K-Ar method. In this method, ^{39}Ar and ^{40}Ar are measured either simultaneously or consecutively via mass spectrometry. The process reduces analysis errors and helps to observe mineral zones and to permit measurement through gradual heating. Applicability of the method or its conformity for samples can be understood during measurement according to the plateau-age assignment rate. Therefore, the method has a low possibility for misapplication. However, the method is costly due to gradual heating, and it requires many corrections for the emerging isotopes. The Ar-Ar method can be applied for a range of 5000 years to 4.6 billion years, which is the age of the Earth.

The method was chosen due to its appropriateness and its widespread use. The samples were collected among the easily distinguished rocks that represent widespread geological units with a potential of yielding valid results. Such samples were abundant in the rock and had a high content of K. Thus, samples P-09 and N-50 were collected from chlorite schists in the Pınarbaşı deposit area, and M-14 and M-15 were collected from the mica schists of Pütürge Metamorphites. These samples are with K_2O content ranging between 2.24–4.64wt %.

The $^{40}Ar/^{39}Ar$ analyses required for age assignment were conducted at the University of Michigan, Department of Geological Sciences. Samples were first exposed to neutron rays for 24 hours in a nuclear reactor. Subsequently, sample particles and standards were analyzed in a laser fusion system with 5 W power and in multiple modes using an Ar ion. The sample particles were first heated gradually. The gas deregulating with heat was cold-purified and was then pumped into a VG-1200S mass spectrometer that was connected to a Daly Detector. Each ^{39}Ar isotope obtained through mass reagents was read 12 times and was normalized according to atmospheric Ar (i.e., $^{40}Ar/^{36}Ar$ =295.5), to ^{36}Ar resulting from ^{37}Ar and ^{37}Cl half life, and to contaminating Ca and K that resulted from nuclear reactions. As a

standard, hornblende MMhb-1 (K-Ar age 520.4 Ma) was used [32]. The neutron-flux parameter "J" was measured at each standard position. In other words, J values were found through interpolation of unknown sample values according to known standard values. The J parameter is calculated using a general equation:

$$J=\frac{e^{\lambda t_m}-1}{\frac{^{40}Ar*}{^{39}Ar}} \quad (3)$$

In this equation,

J= Irradiation flux coefficient,
$^{40}Ar^*/^{36}Ar$= Ratio of isotopes measured on the monitor ($^{40}Ar^*$ means radioactive)
t_m= Monitor flux age,
λ= Total ^{40}K transformation constant and
e= Natural logarithm base (2.718).

Each age result was normalized to 520.4 Ma, which is the K-Ar age of the standard. Error rates for total gas and for plateau age were calculated to be in the range of 1 σ.

The J parameter for $^{40}Ar^*$ and $^{39}Ar_K$ are defined isotopes and were used in the age calculation equation. The equation for t rock or mineral age is as follows:

$$t=\frac{1}{\lambda}.\ln\left[\left(\frac{^{40}Ar*}{^{39}Ar}\right).J+1\right] \quad (4)$$

Here,

t=age (years),
λ=^{40}K total transformation constant,
$^{40}Ar^*=^{40}Ar$ isotope transformed from ^{40}K ("daughter" isotope) and
$^{39}Ar=^{39}Ar$ isotope produced from ^{39}K through neutron activation ("mother" isotope, [59]; [60]; [61]and [62].

Basic Ar values were obtained according to this theoretical basis [19]. These data can be correlated and presented as a f($^{39}Ar/^{40}Ar$, $^{36}Ar/^{40}Ar$) isochrone, for example. Alternately, they can be presented as phases of heating, as demonstrated in (Fig. 17).

The sample data obtained provide two mineral (muscovite) ages in their outlines. Early (or "first age") corresponds approximately to 66 Ma, and the second (or "young age") corresponds approximately to 48 Ma. Therefore,

P-09 sample has an age of approximately 66 Ma, with a plateau age of approximately 100wt % (Fig. 17a).

N-50 sample, as P-09, indicates that it was formed about 66 Ma ago. However, later on, probably about 50 Ma ago, it lost Ar at a significant rate (Fig. 17b). Such distribution of age is peculiar to the loss of Ar through diffusion.

M-14 sample provides a plateau age at about 48 Ma. As seen on the Ca/K and Cl/K diagrams (Fig. 17c), the sample, which resembles a mineral mixture, provides a greater age under high laboratory temperatures.

M-15 sample indicates that it is only approximately 48 Ma old (52 Ma, Fig. 17d).

In brief, the samples analyzed are at least 66 million years of age. However, they have lost Ar due to significant heating at about 48 Ma. This heating was probably due to magmatic activity and tectonic movements resulting from overlapping in the region. The development of ophiolite, the rise of the Maden Complex (Eocene) and the overlapping movements of metamorphic rocks can be given as examples (see [63]). The youngness may be a result of a new metamorphism in the region or of the end of a retrograde metamorphism (i.e., closure heating). The issue may be clarified in future detailstudies.

The geological ages provided above are concordant with previous age assignments in the region. For example, the amphiobolite, biotite and muscovite K-Ar ages of the Pütürge Massif are given as 85, 66 and 47 Ma, respectively [13]. The 66 and 48 Ma ages of M-14 and M-15 mica schist samples from Pütürge Massif, as detected here, are concordant with these results. They also have the same ages as the P-09 and N-50 samples of Malatya Metamorphites in the Pınarbaşı deposit area. Here, it is revealed that the latest geological processes affected both metamorphic units similarly. The first age is associated with the ophiolite overlapping in Campanien, and the second and young age is associated with cooling of muscovite and biotite in the Eocene (cooling ages, [13]).

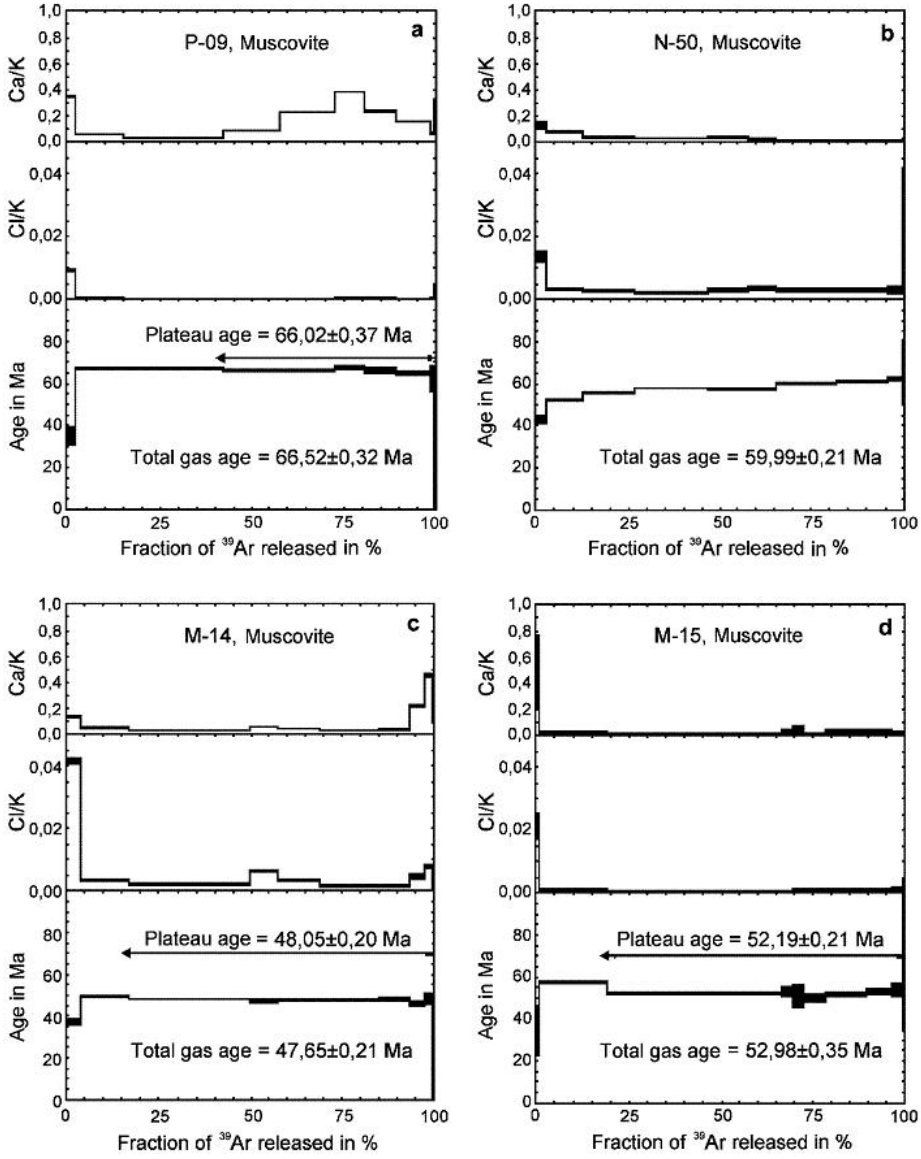

Fig. 17. Distribution of $^{40}Ar/^{39}Ar$ in graduelly heated muscovite samples. Abscissa shows the cummulative partof ^{39}Ar in % and the ordinate the calculatetd age in Ma. The brocken step lines of graphs signifie the heating rank (10 steps =10 heating ranks). The low values of first step left, refers to Ar lost, for example, by difusion. In graph b it is not possible to get a reliable plateau age because of continuous Ar rate (see text, a-d, samples graphs)

The age limits detected here are not considered highly concordant with the age data obtained in Bitlis Massif [64]: 91±9, [65]: 71±28, and [66]: 100 to 70 Ma). These data demonstrate that the Pütürge and Bitlis Massifs were exposed to compression in Late Cretaceous Period at the earliest [13]. Therefore, the "old" heating at 66 Ma (74-56 Ma) in Pütürge Massif and Malatya Metamorphites is associated with this compression.

5. CONCLUSION

Despite numerous geological, mineralogical and geochemical studies conducted over more than 100 years, the formation of "apatite-magnetite deposits" cannot be explained, and no "model of formation" that is generally acknowledged has been put forward.

The Pınarbaşı magnetite-apatite ore deposit that is studied here is a deposit with apatite-magnetite and basic wall rocks. Metamorphism has erased the traces of previous geological process and complicated the synthesis of original development. However, microscopic findings such as the chlorite (sericite) schist wall rock, the laminate structure and the particularly small particles of apatite indicate a sedimentary origin. Geochemical results, such as high Al_2O_3 content and its correlation with K_2O and Ba in the wall rock, the variations of alk-al-c/fm and Niggli values; low Ti and trace-element content in the magnetite also support this view.

According to these findings, a Paleozoic, old, pelitic sedimentation in the Malatya Metamorphites has maintained the formation of alkaline sediments that establish the primary material for chlorite schist wall rock, which is today composed of chlorite, chloritoid, muscovite, biotite, tremolite, epidote and quartz from the Permian period at the latest. The Fe and P that were required for magnetite and apatite enrichment in the deposit were probably accumulatad the media as ions and were settled simultaneously. Therefore, distribution of Fe and P is concordant in the area. The variable concentration of the coming Fe and P resulted in an intercalation of wall rock and ore. The variable concentration also resulted in the ion's decreasing concentration with the depth. The basic material of magnetite, which was shaped through the settlement of increasing sedimentation, was most likely hematite. The basic material of apatite was phosphate minerals.

The increasing temperature in the basin (the last of which was during ophiolite formation in Cretaceous period), the reductive effect of pH and Eh values, the following pressure of at least 0.4 GPa and the metamorphism conditions at 400°C have transformed hematite into magnetite and have transformed the phosphates into apatite. The directed forces of the succeeding metamorphism and compression movements in the east and west directions have led to bending, breaking and overlapping in the deposit, which has given the region its present shape. Although the wall rock was organized through schistosity and foliation, the ore was adapted to array and direction in a massive, banded and dispersed way. Thus, the levels where magnetite was dense were intercalated in the wall rock as a lens. This organized intercalation is indication of sedimentation in a tranquil media. The deposit has undergone at least one regional metamorphosis, which was most likely followed by a retrograde metamorphism. After these geological processes, which erased the former deposit features, the deposit was exposed to an east-west compression and was then pushed over the Eocene-aged Maden Complex. It then took its present shape with later processes of ascending, descending and corrosion.

In brief, according to the results of the study conducted so far, the Pınarbaşı metamorphic ore deposit can be defined as a metamorphic sedimentary iron deposit. Similar deposits are include the Avnik (Bingöl Province) and the Ünaldı (Bitlis Province) deposits in Turkey [11].

These studies, which described a metamorphosed sedimentary formation process for the ore, calculated the total ore reserves to be 69.2 Mt with 28.56wt % Fe and 2.01wt % P_2O_5 tenor [17]. In more recent studies, the combined proved and inferred reserves were determined to be 66.2 Mt with 36.04wt % Fe and 2.07wt % P_2O_5 content [67], whereas [68] are to give 78 Mt with 35.07wt % Fe (for Fe ores over 20wt %) and 1.57wt % P_2O_5 content. The operation of the ore is currently planed for 2016.

This project will provide great savings in foreign exchange by the use of national resources. The production facilities of phosphor, fluor and fertilizer that will be developed alongside the mining shall contribute to development of the Çelikhan District. Finally, the management of iron deposits in Hasançelebi and an iron-steel facility in Malatya may also be considered.

COMPETING INTERESTS

Authors have declared that no competing interests exist.

REFERENCES

1. Frietsch R, Perdahl J-A. Rare earth elements in apatite and magnetite in Kiruna type iron ores and some other iron ores types. Ore Geology Review. 1995;9:489-510.
2. Young EJ, Myers AT, Munson EL. Mineralogy and geochemistry of fluorapatite from Cerro de Mercado, Durango/Mexico. US Geological Survey Prof. Paper 650-D. 1969;84-93.
3. Megaw PKM, Barton MD. The geology and minerals of Cerro de Mercado, Durango,

Mexico. Rock an Minerals. 2010;74(1):20-28.
4. Sillitoe RH, Burrows DR. Feld evidence bearing on the origin of the El Laco Magnetite deposit, northern Chile. Econ. Geol. 2002;97(5):1101-1109.
5. Torab FM, Lehmann B. Magnetite-apatite deposit of the Bafq District, Central Iran: apatite geochemistry and monazite geochronology. Min. Mag. 2007;71(3):347-363.
6. Mokhtari MAA, Zadeh GH, Emami MH. Genesis of iron-apatite ores in Posht-e-Badam Block (Central Iran) using REE Geochemistry. J. Earth Syst. Sci. 2013;122(3);795-807.
7. Erdoğan B, Dora OÖ. Geology and genesis of the apatite-bearing iron deposits of the Bitlis Massif. Proceedings of the International Symposium on the Geology of Tuarus Belt. 1983;96-97.
8. Helvacı C. Apatite-Rich Iron Deposits of the Avnik (Bingöl) Region, Southeastern Turkey. Economic Geology. 1984;79(2):354-371.
9. Aral H. Geology, geochemistry and magnetite-apatite mineralization of of the Avnik area, Genç-Bingöl, SE Turkey. Geologica Utraiectina, Utrecht: Paperbeck; 1986.
10. Çelebi H. Die Magnetit-Apatit-Lagerstätte Avnik/Ost-Türkei. Fortschritte der Mineralogie. 1988;66(2):197-236.
11. Çelebi H. Türkiye apatitli manyetit yatakları: Jeolojisi, jeokimyası ve ekonomik potansiyeli. İstanbul Üniversitesi, Yer Bilimleri Dergisi. 2009;22(1):67-83.
12. Perinçek D. Geological Investigation of the Çelikhan-Sincik-Koçali Area, (Adıyaman Province). Bulletin of the Faculty for Natural Sciences of İstanbul University. 1979;44:127-147.
13. Yazgan E, Chessex R. Geology and tectonic evaluation of the Southeastern Taurides in the Region of Malatya. Turkish Petroleum Geologists Association Bulletin. 1991;3(1):1-42.
14. Bozkaya Ö, Yalçın H, Başıbüyük Z, Özfırat O, Yılmaz H. Origin and evolution of the Southeast anatolian metamorphic complex. Geol. Carpathica. 2007;58(3):197-210.
15. Yiğit Ö. Mineral deposits of Turkey in relation to tethyan metallogeny: Implication for future mineral exploration. Econ. Geol. 2009;104: 19-51.
16. Kuşçu İ, Tosdal RM, Gençalioğlu-Kuşçu G, Friedman R, Ullrich TD. Late cretaceous to middle eocene magmatism and metallogeny of a portion of the Southeastern anatolia orogenic belt, East-Central Turkey. Econ. Geol. 2013;108:641-666.
17. Büyükkıdık H, Aras A. Adiyaman-Çelikhan-Pinarbasi apatite iron mine geology report. Mineral Research and Exploration report 1803 (unpublished); 1984. Turkish.
18. Önal A, Şaşmaz A, Onal A. Pinarbasi (which Çalikh) apatite magnetite ore mineralogy, geochemistry and origin. Geoscience. 2002;40(4):207-226. Turkish.
19. Çelebi H, Helvacı C, Uçurum A. Bulam (Pınarbaşı)/Magnetite Apatite bed of vanadium, rare earths and analyzed for fluorine and economics to investigate. Scientific and Technological Research Council of Turkey, Project YDABAG–101Y119 (unpublished); 2005. Turkish.
20. Çelebi H, Helvacı C, Uçurum A. Apatite-bearing magnetite ore deposit of Pınarbaşı (Adıyaman); geological, geochemical properties and economic potential. Mineral Research and Exploration Bulletin. 2010;141:29-54.
21. Yılmaz Y. New evidence and model on the evolution of the Southeast Anatolien Orogen. Geol. Soc. Am. Bull. 1993;105:251-271.
22. Dilek Y, Imamverdiyev N, Altunkaynak Ş. Geochemistry and tectonics of Cenozoic volcanism in the Lesser Caucasus (Azerbaijan) and the peri-Arabian region: Collision-induced mantle dynamics and its magmatic fingerprint. International Geology Review. 2010;52(4):536-578.
23. Ustaömer PA, Ustaömer T, Gerdes A, Robertson AHF, Collins AS. Evidence of precambrian sedimentation/magmatism and Cambrian metamorphism in the Bitlis Massif, SE Turkey utilising whole-rock geochemistry and U-Pb LA-ICP-MS zircon dating. Gond. Res. 2012;21(4):1001-1018.
24. Yılmaz Y, Yiğitbaş E. SE Anadolu'nun farklı ofiyolitik-metamorfik birlikleri ve bunların jeolojik evrimdeki rolü. Proceedings of the Türkiye 8. Petrol Kongresi. 1990;128-140. Turkish.
25. Yılmaz Y, Yiğitbaş E, Genç C. Ophiolitic and metamorphic assemblages of southeast Anatolia and their significance in the geological evolution of the orogenic belt. Tectonics. 1993;12(5):1280-1297.

26. Işık V. Structure of the Southeast anatolien suture zone, Turkey. American Geophysical Union, Fall Meeting (abstract); 2008.
27. Gözübol AL, Önal M. Malatya-Çelikhan alanının jeolojisi. Scientific and Technological Research Council of Turkey, Project TBAG-647 (unpublished); 1986. Turkish.
28. Westaway R, Arger J. The Gölbaşı Basin, southeastern Turkey: A complex discontinuity in a major strike-slip fault zone. Journal of the Geological Society of London. 1996;153:729-744.
29. Robertson AHF, Parlak O, Rızaoğlu T, Ünügenç Ü, İnan N, Taslı K, Ustaömer T. Tectonic evolution of the South Tethyan ocean: Evidence from the Eastern Taurus Mountain (Elazığ region, SE Turkey). In: Ries AC, Buttler RWH, Graham RH. Deformation of the continental Crust. Geological Socity special publication. 2007;272:231-270.
30. Bucher K, Grapes R. Petrogenesis of metamorphic rocks. 8. Ed. Berlin-Hedelberg: Springer; 2011.
31. Winkler HGF. Petrogenesis of metamorphic rocks. 5. Ed. New York, Heidelberg-Berlin: Springer; 1976.
32. Samson SD, Alexander EC. Calibration of the interlaboratory ^{40}Ar-^{39}Ar dating standard MMhb-1. Chemical Geology. 1987;66:27-34.
33. Sharp ZD. Laser-based microanalytical method for the in situ determination of oxygen isotope ratios of silicates and oxides. Geochimica et Cosmochimica Acta. 1990;54:1353-1357.
34. Vennemann TW, O'Neil JR. A simple and inexpensive method of hydrogen isotope and water analyses of minerals and rocks based on zinc reagent. Chemical Geology. 1993;103:227-234.
35. Valley JW, Kitchen N, Kohn MJ, Niendorf CR, Spicuzza MJ. UWG-2, a garnet standard for oxygen isotope ratios: Strategies for high precision and accuracy with laser heating. Geochimica et Cosmochimica Acta. 1995;59(24):5223-5231.
36. Leake B. The chemical distribution between ortho and para amphilites. J. of Petrology. 1964;5(2):238-254.
37. Mason B, Moore CB. Grundzüge der Geochemie. Stuttgart: Enke; 1985. German.
38. Çelebi H. Ansätze zur Rohstoffwirtschaftlichen Bewertung der Magnetit-Apatit-Lagerstätte Avnik, Ost-Türkei. Erzmetall. 1989;42(2):78-85. German.
39. Pfeufer J. Phosphate in the iron ore deposit of Leonie in Auerbach (Oberpfalz). Trace elements in deposits. Clausthal-Zellerfeld: GDMB publication 80. 1997;41-52. German.
40. Ranjbar M. Dephosphorization of iranian oxide fines by flotation. Erzmetall. 2002;55(11):613-616.
41. Fernandez A, Moro, MC. Origin and depositional envirenment of Ordovician stratiform iron mineralization from Zamora (NW Iberian Pensula). Min. Deposita. 1998;33:606-619.
42. White WM. Geochemistry. Chichester: Wiley-Blackwell; 2013.
43. Stosch H-G. Geochemie der Seltenen Erden. Script zur Vorlesung am Mineralogisch-Petrographischen Institut der Universität zu Kölln 2002; Accessed 23.12.2013. Available: http://institut-seltene-erden.org/wp-content/uploads/2013/11uni-kölln. German.
44. Ekambaram V, Brookins DG, Rosenberg PE, Emanuel KM. Rare-earth elements geochemistry of fluorite-carbonate deposits in Western Montana, USA. Chemical Geology. 1986;54:319-331.
45. Okrusch M, Matthes S. Mineralogie. Berlin-Heidelberg: Springer; 2005. German.
46. Rösler HJ. Lehrbuch der Mineralogie. 4. ed. Leipzig: VEB; 1988. German.
47. Nyström JO, Henriquez F. Magmatic feature of iron ores of the Kiruna type in Chile and Sweden: Ore textures an magnetite geochemistry. Economic Geology. 1994;89:820-839.
48. Çelebi H. Die Genese der Magnetit-Apatit-Lagerstätte Avnik, Provinz Bingöl/Türkei und ihre wirtschaftsgeologische Bewertung. Ph. Thesis, Technical University of Berlin (unpublished).Berlin; 1986. German.
49. Daliran F. The magnetite-apatite deposit of Mishdovan, West Central Iran. Heidelberg: Heidelberger Geowissenschaftliche Abhandlungen 37. 1990. German.
50. Shannon RD. Revised effective ionic radii and systematic studies of interatomic distances in halid and chalcogenides. Acta Crystallographica. 1976;32:751-767.
51. McConnell D. Apatite. Its crystal chemistry, mineralogy, utilization, geologic and

biologic occurences. Vienna: Springer; 1973.
52. Tamish M. Geomathematical and geochemical studies on egypten phosphorite deposits. Berlin: Berliner Geowissenschaftliche Abhandlungen; 1988.
53. Cook JP. Petrology and geochemistry of the phosphate deposits of northwest Queensland, Australia. Economic Geology. 1972;87:1193-1213.
54. Çelebi H, Helvacı C, Uçurum, A. Bulam (Pınarbaşı)/Adiyaman Magnetite Apatite Deposit of. Istanbul: Istanbul University, Turkey Proceedings of the Symposium on Iron Beds. 2005;223-247. Turkish.
55. Aral H. Avnik (Young, Bingol) magnetite-apatite oxygen isotope geothermometry bed. Geoscience. 1986;13:59-62. Turkish
56. Zheng YF. Calculation of oxygen isotope fractionation in metal oxides. Geochimica et Cosmochimica Acta. 1991;55:2299-2307.
57. Zheng YF, Simon K. Oxygen isotope fractionation in hematite and magnetite: A theoretical calculation and application to geothermometry of metamorfic iron-formation. European Journal of Minereralogy. 1991;3:877-886.
58. Brownlow AH. Geochemistry. 2. ed. New Jersey: Prentice Hall, Inc.; 1996.
59. Arehart B. Short course in isotope geochemistry. Sivas: Cumhuriyet University Press; 2005.
60. Stosch HG. Introduction to Isotope Geochemistry. Script to lecture at the Institute of Mineralogy and Geochemistry, University of Karlsruhe (unpublished); 2004. German.
61. Lambert DD, Ruiz J. Application of radiogenic isotopes to ore deposit research and exploration. Rewiev in Economic Geology; 1999.
62. Ottonelb G. Geochemistry. New York: Colombia University Press; 1997.
63. Aktaş G, Robertson AHF. The Maden Complex, SE Turkey: Evoluation of a neo-tethyan active margin. In: Dixon, JE, Robertson (Eds.): The geological evaluation of the Eastern Mediterranean. Geological Society of London, Special Publications. 1984;17:375-402.
64. Helvacı C, Griffin WL. Rb-Sr geochronology of the Bitlis Massif, Avnik (Bingöl) Area, SE Turkey. Geological Society of London, Special Publications. 1984;13:225-265.
65. Göncüoğlu MC. Metamorphism and age of Muş-Kızılağaç Metagranite. Mineral Research and Exploration Bulletin. 1983;99:100.
66. Yılmaz O, Michel R, Vialette Y, Bonhomme M. Reinterpretation of the Rb-Sr isotopic give obtained on metamorphites the southern part of the Massif Bitlis (Turkey). Bulletin Geological Society of Strasbourg. 1981;34:59-73. French.
67. Güneş Ö. Bulam (Adıyaman) Magnetite Apatite bed and reserves, the geology of the calculation. Master Thesis, Firat University (unpublished). Elazig; 1994. Turkish.
68. Sınacı H, Çelebi, H, Alpaslan M, Helvacı C, Uçurum A. Bulam (Pınarbaşı) Çelikhan/ apatite magnetite bearing geological features of Adiyaman and economic potential. Proceedings of the Symposium on the tenth year of Mersin University. 2003;68. Turkish.

Peer-review history:
The peer review history for this paper can be accessed here:
http://www.sciencedomain.org/review-history.php?iid=743&id=22&aid=6605